Petroleum Science 20 (2023) 3379–3393

Contents lists available at ScienceDirect

Petroleum Science

journal homepage: www.keaipublishing.com/en/journals/petroleum-science

Original Paper

Diagenetic evolution and effects on reservoir development of the Dengying and Longwangmiao formations, Central Sichuan Basin, Southwestern China

Lei Jiang [a, b, c, d, *], An-Ping Hu [e, **], Yong-Liang Ou [a, b, c], Da-Wei Liu [f], Yong-Jie Hu [g], You-Jun Tang [d], Peng Sun [d], Yuan-Yuan Liu [h], Zi-Chen Wang [a, b, c], Chun-Fang Cai [a, b, c]

[a] Key Laboratory of Cenozoic Geology and Environment, Institute of Geology and Geophysics, Chinese Academy of Sciences, Beijing, 100029, China
[b] Innovation Academy for Earth Science, Chinese Academy of Sciences, Beijing, 100029, China
[c] College of Earth and Planetary Sciences, University of Chinese Academy of Sciences, Beijing, 100049, China
[d] College of Resources and Environment, Yangtze University, Wuhan, Hubei, 430100, China
[e] PetroChina Hangzhou Research Institute of Geology, Hangzhou, Zhejiang, 310023, China
[f] Petroleum Exploration and Production Research Institute, SINOPEC, Beijing, 100083, China
[g] Sinopec International Petroleum Exploration and Production Corporation, Beijing, 100029, China
[h] Institute of Sedimentary Geology, Chengdu University of Technology, Chengdu, Sichuan, 610059, China

ARTICLE INFO

Article history:
Received 8 March 2023
Received in revised form
30 May 2023
Accepted 30 September 2023
Available online 8 October 2023

Edited by Jie Hao and Teng Zhu

Keywords:
Carbonate reservoir
Diagenesis
Dolomitization
Meteoric water
Oil charge
Hydrothermal fluids
Tectonic-driven fractures
Deep to ultra-deep exploration

ABSTRACT

The deeply buried Lower Cambrian Longwangmiao Formation and Upper Ediacaran Dengying Formation from the Sichuan Basin, China, have a total natural gas reserve up to 3×10^{12} m^3. The complex diagenetic evolution and their impacts on the present-day reservoir quality have not been systematically elucidated, hampering the current exploration. Crucially, the integration and comparation diagenetic study on these two formations, which may be able to shed new lights on reservoir formation mechanism, are yet to be systemically evaluated. By compiling geochemistry data, including carbonate U-Pb ages and petrophysics data, coupled with new petrology, trace elements, and strontium isotope data, of various types of diagenetic carbonates, this study aims to decipher the potential links between diagenesis and reservoir development of both formations. Intriguingly, similar diagenetic sequence, which contains five distinctive dolomite phases, is established in both formations. The matrix dolomite (D1) and early dolomite cement (D2) were likely formed by reflux dolomitization, as inferred by their nearly syn-depositional U-Pb ages and elevated $\delta^{18}O$ caused by seawater evaporation. The subsequent moderate burial dolomite cement (D3) was most plausibly the product of burial compaction as indicated by its lighter $\delta^{18}O$ and slightly younger U-Pb ages compared with D1 and D2. Whereas deep burial dolomite cements (D4 and D5) yield markedly depleted $\delta^{18}O$, elevated $^{87}Sr/^{86}Sr$, along with much younger U-Pb ages and higher precipitation temperatures, suggesting that they were likely linked to hydrothermal fluids. Despite the wide occurrence of meteoric and organic acids leaching and thermochemical sulfate reduction, they may have only played a subsidiary role on these reservoirs development. Instead, superior reservoir quality is tightly linked to tectonics as inferred by higher reservoir quality closely related to the well-developed fractures and faults filled with abundant hydrothermal minerals. Notably, good reservoirs in both formations are mainly attributed to high permeability caused by tectonics. Hence, this new contribution emphasizes the crucial role of tectonics on spatially explicit reservoir prediction of deep to ultra-deep (up to > 8000 m) carbonates in the Sichuan Basin, as well as other sedimentary basin analogues in China.

1. Introduction

Deeply burial carbonate reservoirs in China have gained increasing attentions because of their great potentials in energy

* Corresponding author. Key Laboratory of Cenozoic Geology and Environment, Institute of Geology and Geophysics, Chinese Academy of Sciences, Beijing, 100029, China.
** Corresponding author.
E-mail addresses: lei.jiang@mail.iggcas.ac.cn (L. Jiang), huap_hz@petrochina.com.cn (A.-P. Hu).

https://doi.org/10.1016/j.petsci.2023.09.025

resource explorations, i.e., petroleum and geothermal water in several major sedimentary basins, i.e., Sichuan, Tarim, Ordos, Bohai Bay basin (Zhao et al., 2014; Zhu et al., 2015; Liu et al., 2016; Wei et al., 2022). Under deep subsurface condition, reservoir characterization and prediction are of central importance for reserve appraising of those energy resources. Notably, the formation of superior carbonate reservoir under deep burial conditions is jointly controlled by preferential sedimentary facies, i.e., shoal and reef, and profitable diagenetic alterations, i.e., karstification, dolomitization, hydrothermal, and fracturing (Mazzullo and Harris, 1991; Saller and Henderson, 1998; Heydari, 2000; Davies and Smith Jr, 2006; Ehrenberg et al., 2012; Jiang et al., 2018c; Shen et al., 2022).

Whether mesogenesis diagenesis could improve carbonate reservoir quality under relative closed diagenetic systems is on hot debating (Ehrenberg et al., 2012; Hao et al., 2015; Jiang et al., 2018a). Under deep burial conditions, carbonate reservoir quality has been tightly linked to the deposition of sulfates and their dissolution and reduction with petroleum at elevated burial temperatures (Mazzullo and Harris, 1991; Jiang et al., 2018a, 2018c; Jiang, 2022). However, the impacts of sulfate reductions on carbonate reservoirs of late Ediacaran to early Cambrian ages may play a subsidiary role on reservoir development (Liu et al., 2021; Xu et al., 2022; Hu et al., 2023) due mainly to lacking of evaporites deposition. Other factors, such as sea-level fluctuations and faulting events related to tectonics have been tied to deep burial carbonate reservoir formation (Xiao et al., 2020a; Jiang et al., 2022b; Shen et al., 2022), while ultra-deep oil and gas accumulations were commonly linked to mountain front-foreland basin transition zones (Xiao et al., 2020b).

The Upper Ediacaran Dengying Formation and Lower Cambrian Longwangmiao Formation from the Sichuan Basin, China, which have been completely dolomitized, contain enormous natural gas resource, with the maximum reserve of 3×10^{12} m^3 (Yang et al., 2016; Hu et al., 2020b; Liu et al., 2021; Xu et al., 2022; Li et al., 2023). Previous studies have emphasized the crucial role of karstification (Tan et al., 2021; Xu et al., 2022; Yan et al., 2022) and tectonic-related hydrothermal fluids (Zhao et al., 2014; Feng et al., 2017; Shen et al., 2021; Qiao et al., 2022; Su et al., 2022; Li et al., 2023) on the formation of these reservoirs. Although thermochemical sulfate reduction (TSR) has occurred within these reservoirs (Liu et al., 2016, 2021), its effect on reservoir quality enhancement may be insignificant (Xu et al., 2022). However, the systematic comparison of diagenetic evolution between these two formations are lacking, such as how the differentiated karstification, seawater chemistry (i.e., Mg^{2+} and SO_4^{2-}), and environment forces impact on the initial minerology and subsequent diagenesis, which may be crucial in reservoir development.

During the late Ediacaran to early Cambrian transition, the global seawater and atmospheric compositions, marine redox and life, and climate witness dramatic changes (Wood et al., 2017; Jiang et al., 2022a). The Anyue gas field, one of the biggest exploit gas fields in China, containing both the Longwangmiao Formation and Dengying Formation, thus offering us a great opportunity to test above assumptions. The analyzed data from this study consists of: i) compiled geochemical data, including carbon, oxygen, strontium isotopes, and temperatures, as well as petrophysical data, including core plugs porosity and permeability, and ii) newly measured petrology and geochemistry data, such as Fe, Mn, Sr contents, and some strontium isotopes, of dolostone reservoirs in both formations. The outcomes from this study seems to emphasize the crucial role of tectonics and their associated fluids activities on enhancing carbonate reservoir quality under deep burial conditions.

2. Geological setting

The Sichuan Basin, a stable craton basin on the Yangtza Platform, which is located in the Sichuan Province, southwestern China, covers an area of about 2.3×10^5 km^2 (Hu et al., 2020b; Liu et al., 2021; Wei et al., 2022). It is structurally divided into three subtectonic units, which is bound by the Micang and Daba Mountains to the north, the Dalou and Qiyue Mountains to the east, the Emei Mountains to the south, and the Longmen Mountains to the west (Fig. 1a). From the Ediacaran to Middle Triassic, it was a Cratonic basin and received marine deposition. Giant gas fields were found mainly in the paleo-uplift structure in the Gaoshiti-Moxi region in the both formations (Fig. 1a). From bottom to up, the Ediacaran to Cambrian units in Central Sichuan Basin are represented by the Doushantuo Formation (Z_2ds), Dengying Formation ($Z_2dn^{1\text{-}4}$), Qiongzhusi Formation (ϵ_1q), Canglangpu Formation (ϵ_1c), Longwangmiao Formation (ϵ_1l), Gaotai Formation (ϵ_2g) and Xixiangchi Group ($\epsilon_{2\text{-}3}x$) (Fig. 1b).

The Dengying Formation, with thickness mainly between 200 and 900 m, could be subdivided into four sections (Member I to IV from bottom to up; Fig. 1b) based on lithology changes (Hu et al., 2020b; Wei et al., 2022). Member I is consisted mainly of mudstone, sandstone, and conglomerate, and interlayered with few dolomite beds. Member II is mainly composed by microbial dolomite interlayered with few grain-dolomite. Microbialites in Member II are mainly thrombolites and stromatolites associated with crystalline dolomite layers. While Member III is dominated by brown siltstone, black mudstone and micrite dolomite. Member IV is also consisted mainly of microbial dolomite, but commonly associated with crystalline dolomite and quartz. In general, Member I and III are characterized by mixed clastic and carbonate rock deposited at slope facies, whereas Member II and IV are typical platform margins and intra-platform carbonate depositions where the main reservoirs are commonly found. Few gypsum is locally observed within dolomicrite at intertidal environments (Hu et al., 2020b).

The overlying Qiongzhusi Formation from the lowest Cambrian strata are mainly composed by thick gray mudstone and black shale layers, which is overlapped by dolomudstone and mudstone from the deposition of Canglangpu Formation. The Longwangmiao Formation, where the main reservoir of the Lower Cambrian units located, mainly consists of granular, oolitic, and lagoonal silt fine-crystalline dolomite of shallow slope carbonate ramp facies (Liu et al., 2021). The subsequent deposition of Gaotai Formation is characterized by typical shallow water, mixed carbonate and clastic rocks, while the following depositional of Xixiangchi Group is dominated by a set of thick dolostone successions (Fig. 2) (Fu et al., 2020).

During the late Neoproterozoic to early Cambrian, the Yangtze block was evolved from rifting related to accelerated breakup of the Rodinia supercontinent into a passive continental margin by extensional tectonics. The first episode of Tongwan movement has led to a transient uplift during the transition to second-third member of the Dengying Formation deposition. The following burial-thermal history is quite similar (Fig. 2a) within both formations, which have been buried to $\simeq$ 1500–3000 m during the early Cambrian to early Carboniferous before being uplifted to near surface conditions ($\simeq$ 300–700 m) at the Caledonian orogeny. Subsequently, a rapid and continuous burial stage occurred, leading to both formations reached the maximum depths of $\simeq$ 6000–7000 m during the late Jurassic to early Cretaceous. A Cenozoic uplifting event has brought both formations to the

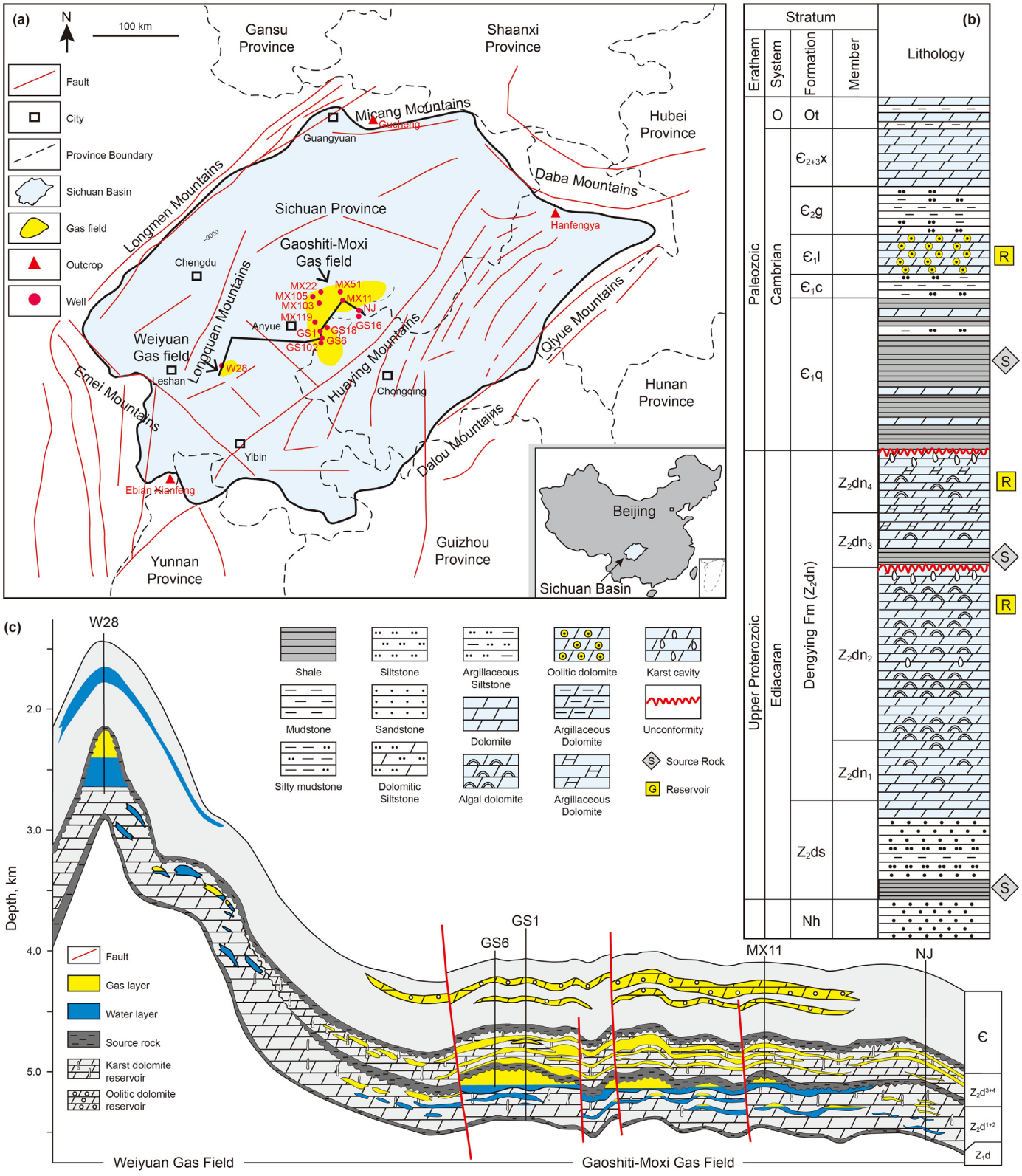

Fig. 1. (a) Regional geological map showing the tectonic elements, locations of studied gas fields, wells and outcrops of the Central Sichuan Basin. (b) Stratigraphy, lithology, and potential source rocks and reservoirs of the Gaoshiti-Moxi gas field. (c) Cross-section (solid black line in a) from the Weiyuan gas field to Gaoshiti-Moxi gas field. Modified after Su et al. (2022).

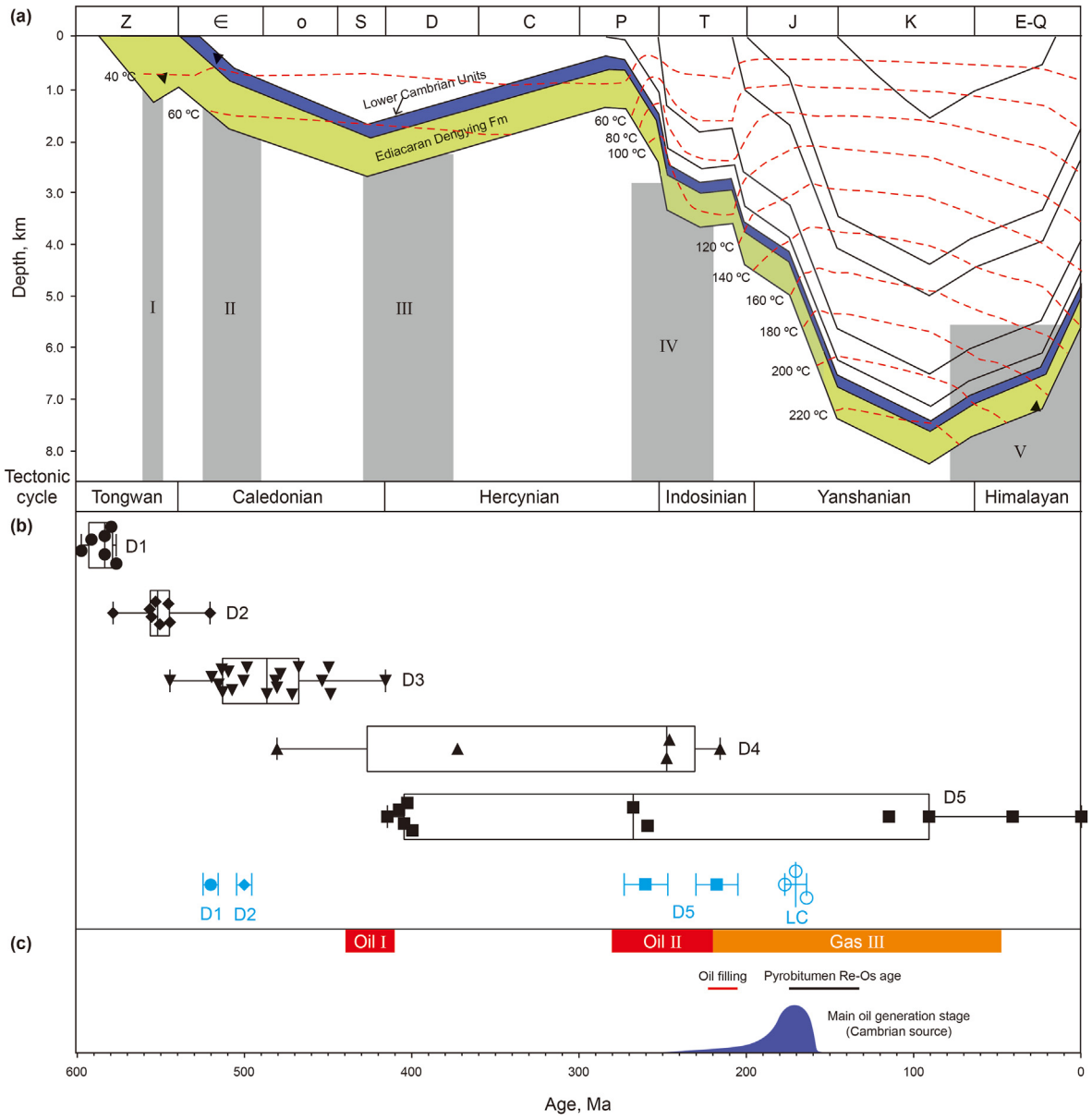

Fig. 2. (a) Typical burial and paleo-temperature history constructed from the Gaoshiti-Moxi region in Central Sichuan Basin, modified after Liu et al. (2018). The Dengying Formation is in green while the Lower Cambrian units is in purple. Gray bands marked as I to V represent five fracturation events. (b) Age model for diagenetic carbonates in the Dengying Formation (in black) and Longwangmiao Formation (in blue) is constrained by compiled carbonate U-Pb ages. (c) Timing for major oil and gas charging events (red and orange bar) is mainly modified after Shen et al. (2021), oil filling timing (red line) constrained by fluid inclusion while timing for gas generation due to thermal cracking of oil as constrained by pyrobitumen Re-Os age, modified after Su et al. (2020).

current burial depths of ≃ 4500–5500 m. Multistage fractures related to aforementioned tectonics along with hydrothermal fluid activities and mineral assemblages (dominated by carbonates) were present in both formations, providing materials for dating the tectonic events (Fig. 2b).

The source rocks for these gas fields are predominated by the Lower Cambrian Qiongzhushi shales, although few may have contributed by shaly carbonates from the Upper Ediacaran Dengying Formation, and shales from the Lower Ediacaran Doushantou Formation (Fig. 1b) (Zhu et al., 2015, 2022; Liu et al., 2016; Shi et al., 2018; Li et al., 2021). The first episode of paleo-oil charging in the Dengying Formation occurred during the late Ediacaran to early Cambrian, with its source rock most likely derived from the underlying Ediacaran Doushantuo shales (Su et al., 2022). The main source rocks in the study area reached the early maturation and started oil generation during the Ordovician-Silurian interval, followed by a major oil charging event during the middle Silurian to early Devonian (Fig. 2c). After a long period of burial ceasing due to the Caledonian uplift from the early Devonian to middle Permian (Fig. 2a), a quick burial stage occurred which resulted in a rapid maturation evolution of source rocks and a peak oil generation during the late Permian to Triassic. Subsequently, gas charging by cracking of oils and generation of pyrobitumen occurred during the late Triassic to early Cenozoic (Fig. 2c). The timing for oil and gas generation based on basin modelling of the Lower Cambrian Qiongzhusi shales broadly coincides with the ages constrained by temperature data obtained from aqueous fluid inclusions associated with oil inclusions and bitumen Re-Os isochron age (Fig. 2c).

3. Samples and methods

We complied the published petrophysical data (porosity and permeability; $n = 1072$), and geochemistry data, including, carbon and oxygen isotopes ($n = 687$), strontium isotope ($n = 125$) and temperature data ($n = 195$) obtained from both fluid inclusion and clumped isotopes measurement, of dolomites from both formations. The carbon and oxygen data of several typical time equivalent carbonate reservoirs from other continents, such as Oman and Siberian, were also compared. Additionally, an age model for diagenetic evolution was constrained by the compiled U-Pb age data ($n = 55$, mostly from the Dengying Formation) of various types of diagenetic dolomites and one late-stage calcite. The compiled data along with their sources are listed in the supplementary data file.

More than 200 core samples from 28 wells containing the Dengying Formation and/or Longwangmiao Formation were collected. 100 polished 25 μm thin sections were prepared for petrology and geochemical analysis. The Alizarin-Red solution was used to differentiate calcite and dolomite mineral. Petrology observatories were performed under polarized light microscope and Relion III CL model cathodoluminescence with the beam voltage of 16.3 kV and the beam current of 325 μA. Selected slices were further observed under scanning electron microscopy (SEM) by using the Nova NanoSEM 450 instrument equipped with an energy spectrometer (X-ray) for semi-quantitative mineral analysis.

The electron probe (EMPA) method was used to analyses trace elements of carbonate rocks at the institute of Geology and Geophysics, Chinese Academy of Sciences (IGGCAS). The instrument model is JAX-8100, the accelerating voltage was 15 kv, the probe current was 10 nA, and the test beam spot size was 20 μm. Eleven elements were selected (MgO, CaO, MnO, FeO, BaO, SrO, SiO_2, Al_2O_3, Na_2O, K_2O and TiO_2), with the test time of 20 s for each element with a 10 s gap background time between each measurement. Elements data verification has been done by using spi mineral standard.

Strontium isotope was analyzed ($^{87}Sr/^{86}Sr$) on various types of dolomites at IGGCAS following the methods of Liu et al. (2021). Briefly, approximately 40–50 mg microdrilled dolomite sample was dissolved in 0.2 mol/L HCl at 80 °C for 4 h. The solution was passed through an ion exchange column to obtain the Sr solution, followed by $^{87}Sr/^{86}Sr$ isotope measurement on the Finnigan MAT-262 thermal ionization mass spectrometer. The calibration of strontium isotopes is relative to the NBS-987 standard, and the standard sample has an average value of 0.7103. The standard deviation (2σ) of $^{87}Sr/^{86}Sr$ during the determination was less than 0.000024.

4. Results

4.1. Petrography

The grain components are distinctive in each formation. They are dominated by ooids and peloids in the Longwangmiao Formation (Fig. 3), whereas characterized by microbilites-dominated peloids in the Dengying Formation (Fig. 4). Pore spaces in both formations are mainly represented by solution-enlarged pores (Fig. 3a-c; Fig. 4a, b).

Five types of dolomites are identified in both formations (Figs. 3 and 4). Dolomite matrix (D1), which is consisted mainly of dolomicrite, represents the initial dolomitization event (Fig. 3c; Fig. 4a). Early dolomite cement (D2), commonly displays dull red CL color (Fig. 3d; Fig. 4c), and occurs mainly as fibrous cement in the Dengying Formation while as bladed cement at the edges of some pore spaces in the Longwangmiao Formation. Medium-to coarse-crystalline dolomite cement (D3), that grew on top of D2, commonly displays bright red under CL in both formations. D3 has relatively large crystal sizes mainly between 100 and 500 micron (μm) and up to several millimeter (mm), containing few petroleum-bearing fluid inclusions (Fig. 3d, e; Fig. 4d). An irregular interface between D2 and D3 (Fig. 3d; Fig. 4d, e) is locally observed. Saddle dolomite cement (D4), commonly occurs as fracture fillings in association with fluorite (Li et al., 2023), and displays non-luminescence under CL. The crystal sizes of D4 varying from 300 μm and up to several micrometers (Fig. 3f; Fig. 4c, d). Medium-to coarse-crystalline dolomite cement (D5), which is commonly associated with coarse-crystalline calcite and quartz cements, represents a very late pore-filling phase (Fig. 3h, i; Fig. 4f).

4.2. Geochemistry data

4.2.1. Carbon and oxygen isotope geochemistry

The complied carbon and oxygen data of varying diagenetic carbonates are positively related with each other (Fig. 5a, b) in both of the Longwangmiao Formation (Ren et al., 2017, 2019; Fu et al., 2020; Zhang et al., 2020; Liu et al., 2021; Wang et al., 2021) and Dengying Formation (Feng et al., 2017; Hu et al., 2020a, 2020b, 2021; Xu et al., 2022). In general, $\delta^{13}C$ values of different carbonate phases display a narrow range mainly between −3 and 1‰ (average at −1‰, SD = 0.87‰, $n = 208$) in the Longwangmiao Formation, while between 0 and 5‰ (average at 3‰, SD = 2‰, $n = 184$) in the Dengying Formation. By contrast, much wider $\delta^{18}O$ range of dolomites present in both formations: ranging from ≃ ca. −11 to −4‰ (average at −7.2‰, SD = 3.5‰, $n = 208$) in the Longwangmiao Formation, and from ≃ −13 to 0‰ (average at −7.5‰, SD = 3.1‰, $n = 184$) in the Dengying Formation. Note that the early diagenetic dolomites (D1 and D2) from the Dengying Formation are much more enriched in ^{18}O than the ones from the Longwangmiao Formation (Fig. 5a, b). Carbonates from typical time-equivalent dolostone reservoir with abundant evaporites deposition from other continents yield much wider and lighter $\delta^{13}C$ values (≃ −10 to 5‰, average at −0.3‰, SD = 4.0‰, $n = 295$), but similar positive $\delta^{18}O$ values (≃ −8 to 0‰, average at −4.7‰, SD = 2.0‰, $n = 295$) of D1 and D2 dolomites compared with the ones from this study (Pokrovsky et al., 2011; Bergmann et al., 2018; Kochnev et al., 2018).

4.2.2. Strontium isotope geochemistry ($^{87}Sr/^{86}Sr$)

In general, $^{87}Sr/^{86}Sr$ isotope ratios for various types of dolomites yield a wide range, from 0.7095 to 0.7369, average at 0.7114 (SD = 0.0044, $n = 58$), in the Longwangmiao Formation, and from 0.7085 to 0.7129, average at 0.7105 (SD = 0.0012, $n = 66$), in the Dengying Formation. Few D1 and D2 dolomites display a relative narrow, coeval seawater $^{87}Sr/^{86}Sr$ isotopic range between 0.7084 and 0.7092 (Montañez et al., 2000; Halverson et al., 2007). By contrast, most D1 and D2 dolomites in both formations yield markedly elevated $^{87}Sr/^{86}Sr$ ratios (0.7094–0.7116). A broadly increasing trend of $^{87}Sr/^{86}Sr$ ratios from D3 to D5 are present in both formations, with higher $^{87}Sr/^{86}Sr$ ratios present in the Dengying Formation compared with the Longwangmiao Formation (Fig. 6).

4.2.3. Temperature data for diagenetic minerals

The compiled temperatures that documented from different diagenetic minerals in both formations (Fig. 7) were obtained from clumped isotopes (Jiang et al., 2022b) and fluid inclusion microthermometric analysis (Feng et al., 2017; Hu et al., 2020a; Liu et al., 2021; Xu et al., 2022). D1 and D2 dolomites in both formations display relative low temperatures (mostly < 50 °C) (Fig. 7), being consistence with their near-surface diagenetic conditions (Jiang et al., 2022b). D3 dolomites in the Dengying Formation yield temperatures ranging mainly from 100 °C to 150 °C, average at ≃

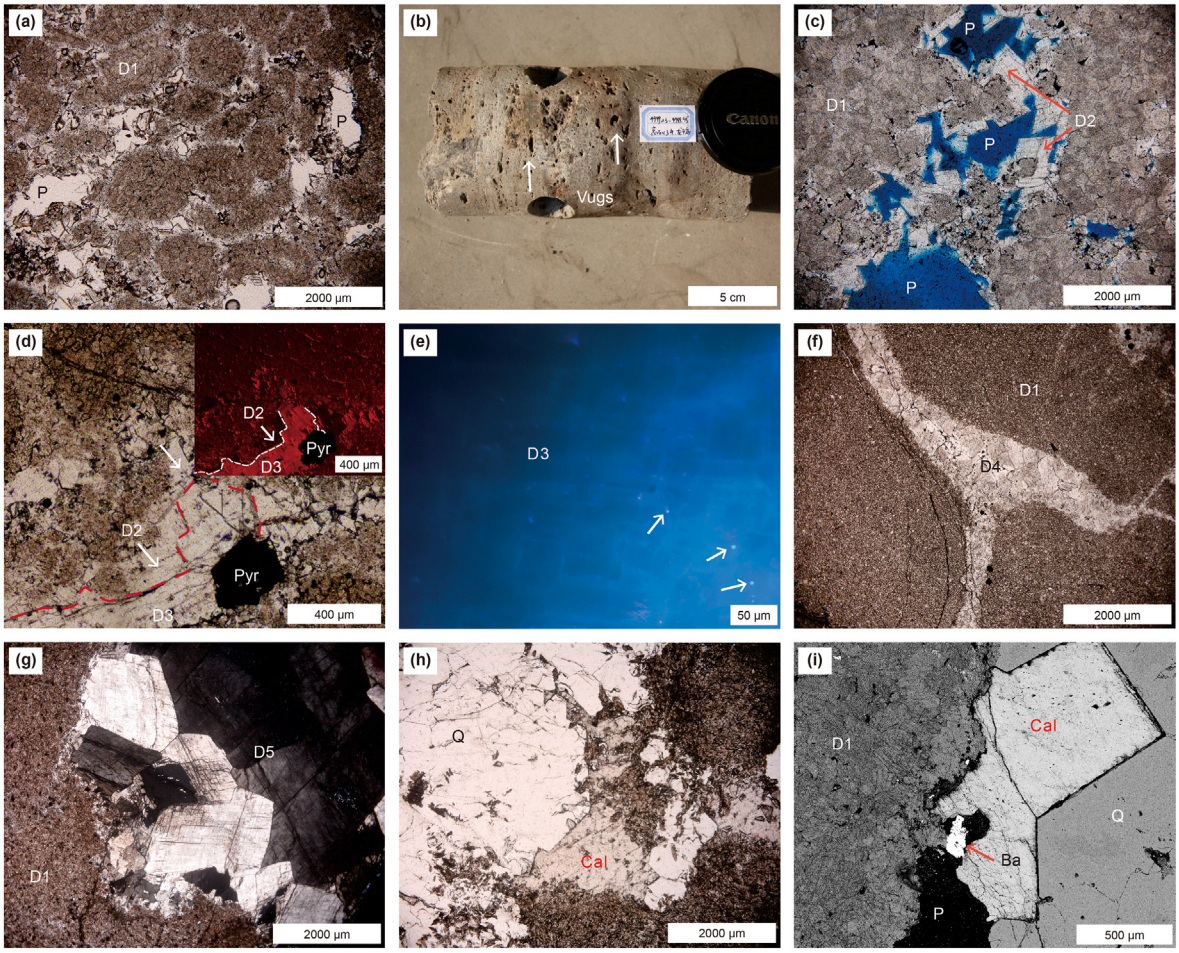

Fig. 3. Microphotographs showing the main diagenetic products in the Longwangmiao Formation. (a) Oolitic shoal facies rich in inter-particle pore spaces, well MX39, depth 4843.5 m; (b) abundant vuggy pores is observed in cores, well GS113, depth 5000.0 m; (c) medium crystalline limpid dolomite cement (D2), well GS10, depth 4619.7 m; (d) medium poikilitic dolomite cement (D3) grew on top of D2, showing bright red CL color, well MX21, depth 4662.1 m; (e) fluorescent oil inclusions in D3 from (d); (f) medium to coarse dolomite vein (D4), well MX11, depth 4875.1 m; (g) coarse rhombic dolomite (D5) grew in pore spaces, well MX23, depth 4806.0 m; (h) later stage calcite cement (Cal) precipitated after quartz cement (Q), well MX41, depth 4816.9 m. (i) late-stage dissolution pore (P) in (h).

120 °C (Fig. 7b). By contrast, hydrothermal dolomites (D4 and D5) and late calcites yield elevated precipitation temperatures lying mainly between 130 °C and 150 °C in the Longwangmiao Formation (Fig. 7a), while between 130 °C and 200 °C (mostly > 150 °C) in the Dengying Formation (Fig. 7b). Some quartz cements in the Longwangmiao Formation yield elevated temperatures mainly between 180 °C and 200 °C (Fig. 7a).

4.2.4. Trace element concentrations

The trace element contents for different types of dolomites in both formations are summarized in Fig. 8 and Table 1. Generally, D1 dolomites have similar Fe (average at ≃ 1100 ppm) and Sr (average at ≃ 200 ppm) concentrations in both formations. While distinctive Mn concentrations of D1 dolomites are observed between the Longwangmiao Formation (average at 434 ppm) and Dengying Formation (average at 257 ppm). D2 dolomites in both formations display relatively low Fe and Sr concentrations while similar Mn concentrations compared with D1 dolomites. Notably, Fe and Mn contents of D3 and D4 dolomites are markedly higher in the Longwangmiao Formation than that of the Dengying Formation, whereas a reversed trend is present in D5 dolomites. From D1 to D5, a broadly decreasing trend of Sr contents along with a general increasing trend of Fe and Mn content, are observed in both formations (Fig. 8). However, a sharp decrease of Fe and Mn contents from D4 to D5 is observed in the Longwangmiao Formation.

4.2.5. U-Pb ages of diagenetic carbonates

The compiled U-Pb age data are predominantly documented from different types of dolomites in the Dengying Formation (Fig. 2b) (Shen et al., 2021; Jiang et al., 2022b; Qiao et al., 2022; Su et al., 2022; Gu et al., 2023). The U-Pb ages of D1 dolomites range from 598 ± 24 Ma to 577 ± 12 Ma, average at 586 ± 8 Ma (n = 6), well falling within the Ediacaran Era. D2 dolomites yield slight (average ≃ 35 Ma) younger U-Pb ages (from 521 ± 21 Ma to 557 ± 11 Ma, average at 551 ± 16 Ma; n = 8) than the ages of D1 dolomites, still failing within the late Ediacaran period. The majority U-Pb ages of D3 dolomites fall mainly between the Cambrian and Ordovician, average at 488 ± 31 Ma (n = 19). By contrast, D4 and D5 dolomites yield much younger U-Pb ages between 481 ± 12 Ma and 216 ± 7 Ma (average at 313 ± 112 Ma; n = 5), and between 415 ± 16 Ma and 0 ± 11 (average at 255 ± 174 Ma; n = 10), respectively. Additionally, two D5 dolomites yield U-Pb ages of 261 ± 13 Ma and 219 ± 12 Ma, and late calcite yield U-Pb age of 171 ± 7 Ma, in the Lower Cambrian Longwangmiao Formation (Fig. 2b) (Li et al., 2023).

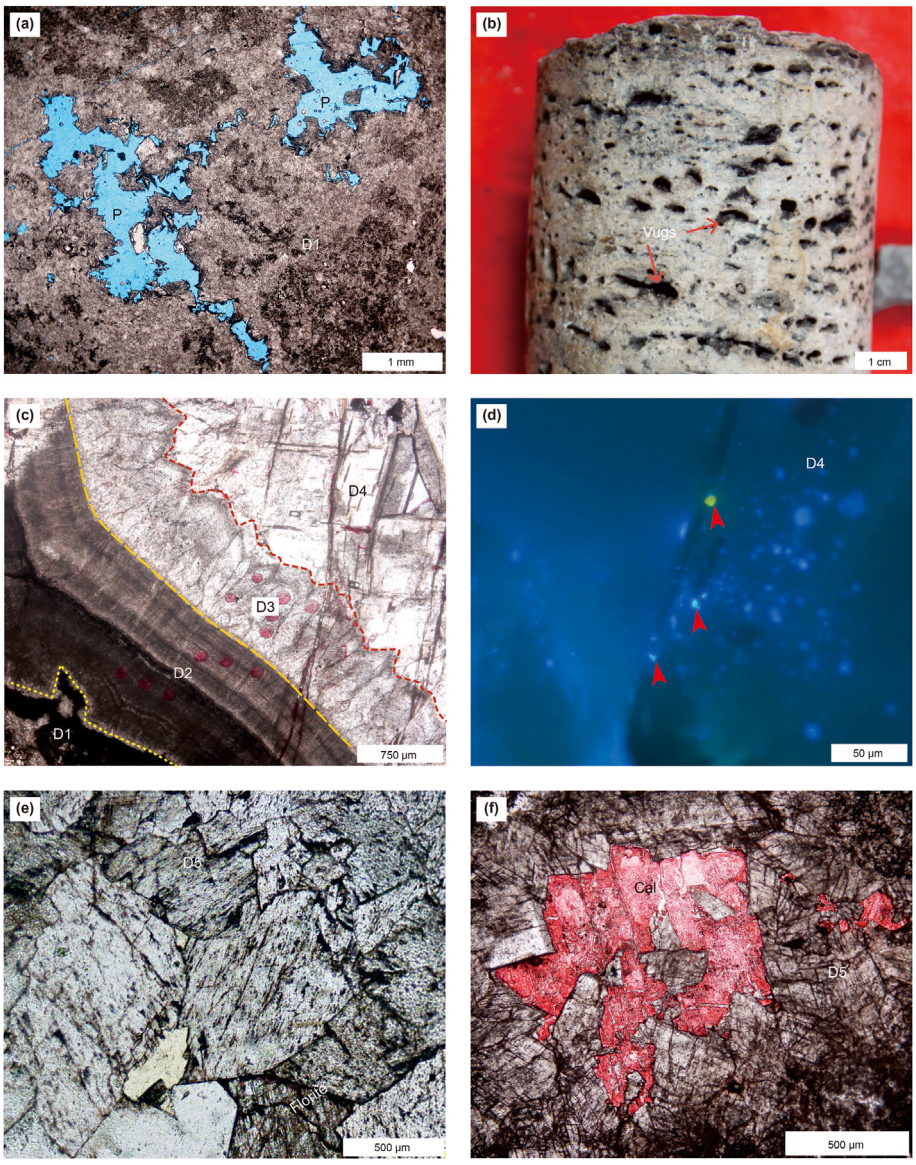

Fig. 4. Microphotographs showing the main diagenetic products in the Dengying Formation. (a) Vuggy pores in microbiallite consists of D1 dolomite, well GK1, depth 5151.5 m; (b) stratiform framework pores in thrombolytic dolostone matrix, well MX52, depth 5568.7 m; (c) fibrous dolomites (D2) are overlined by bladed dolomite cements (D3) and medium to coarse crystalline dolomite cement (D4) in microbiallite reefal facies, well MX9, depth 5457.4 m; (d) hydrocarbon inclusions with blue or yellow fluorescence color in DC3 dolomite; (e) late saddle dolomite (D5) and fluorite minerals, well GK1, depth 5406.0 m; (f) later calcite cements (Cal) precipitated after D5, well GK1, depth 5406.0 m.

4.3. Porosity and permeability data

In general, the compiled porosity (from 0 to 12%) and permeability (from 10^{-4} to 10^{3} mD) of dolomite samples, with 1810 data from the Dengying Formation and 1767 data from the Longwangmiao Formation, yield similar distribution rang and pattern (Fig. 9) (Yang et al., 2016; Zhou et al., 2016; Luo et al., 2017; Shen et al., 2018; Hu et al., 2020b; Liu et al., 2021; Wei et al., 2022). Group I pattern displays relative low porosities ($\simeq$ 1–6%) and high permeabilities ($\simeq$ 10^{-1} to 10^{2} mD), while Group II pattern displays a wider porosity range (~1–10%) with relatively low permeabilities ($\simeq$ 10^{-3} to 10^{2} mD). Majority of porosity data (92.4% for the Longwangmiao Formation and 84.9% for the Dengying Formation) is below 6%, and permeability data (83.6% for the Longwangmiao Formation and 63.8% for the Dengying Formation) is below 1 mD (Fig. 10). Note that the data percentage of high porosity (6–10%) and high permeability (10^{0}–10^{2} mD) in the Dengying Formation is about twice more than that in the Longwangmiao Formation (Fig. 10) (Hu et al., 2020b; Liu et al., 2021; Wei et al., 2022; Xu et al., 2022). Notably, coupling of fractures development and elevated reservoir quality is present in both formations (Fig. 11).

5. Discussion

5.1. Comparing of digenetic evolution model in both formations

This new investigation allows to build the most comprehensive diagenetic sequence model for the Longwangmiao Formation and Dengying Formation (Fig. 12) based on the integrating of detailed petrology and diagenesis studies (Hu et al., 2020b, 2023; Liu et al., 2021; Su et al., 2022; Xu et al., 2022), along with diagenetic evolution age model (Fig. 2b, c) established by compiled carbonate U-Pb age data (Shen et al., 2021; Jiang et al., 2022b; Qiao et al., 2022; Su et al., 2022; Gu et al., 2023). Note that the oil and gas charging

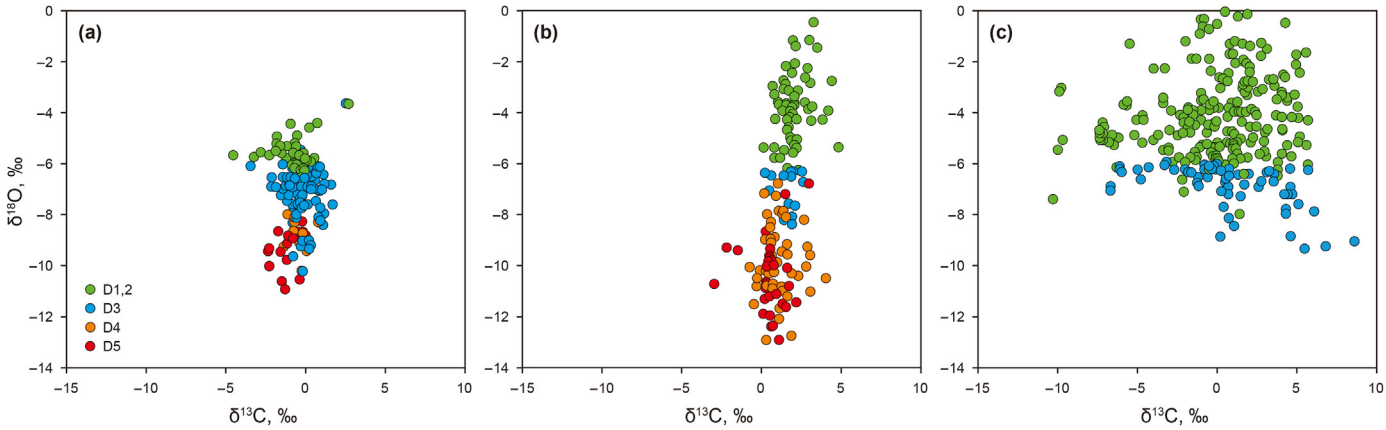

Fig. 5. Compiled $\delta^{13}C$ and $\delta^{18}O$ for different diagenetic carbonate phases in the Longwangmiao Formation (a), Dengying Formation (b), and several global time-equivalent dolostone reservoirs rich in evaporites (c).

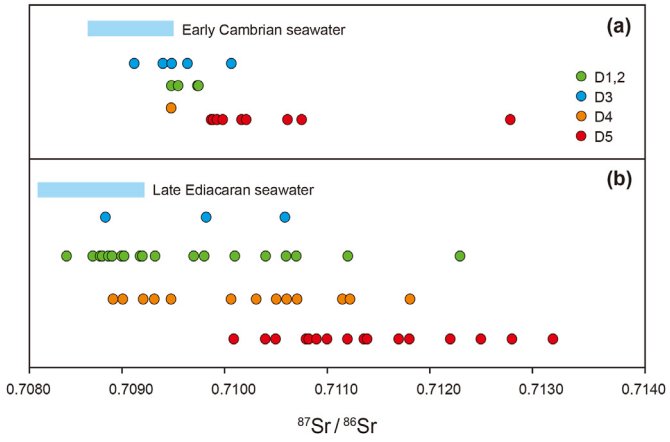

Fig. 6. Compiled $^{87}Sr/^{86}Sr$ ratios for different type of dolomites in the Longwangmiao Formation (a) and Dengying Formation (b). Blue bars showing the $^{87}Sr/^{86}Sr$ value range of coeval seawater. Data sources of $^{87}Sr/^{86}Sr$ are listed in the supplementary data file.

timing as constrained by basin modelling, carbonate U–Pb dating and bitumen Re–Os dating (Su et al., 2020, 2022), as well as temperature data (Fig. 7) obtained from fluid inclusion microthermometry and clumped isotope analysis, are also included.

After initial limestone deposition, an early stage of reflux dolomitization may have occurred due to the evaporation of seawater in restricted facies, which allowed D1 dolomite precipitation in both formations (Liu et al., 2021; Jiang et al., 2022b). Reflux dolomitization could have been more intensive in the Dengying Formation than the Longwangmiao Formation, as inferred by the elevated $\delta^{18}O$ values in D1 dolomites (Fig. 13c), which is positively linked to the extent of seawater evaporation under restricted environments, such as sabkha and lagoon (Saller and Henderson, 1998; Jiang, 2022).

Early dolomite cementation that related to evaporation of seawater occurred nearly syn-depositional or slightly postdated the matrix dolomitization in both formations (Liu et al., 2021; Jiang et al., 2022b; Xu et al., 2022). For instance, fibrous dolomite cements (D2) precipitation in the Dengying Formation were ≃ 30 Ma postdated the matrix dolomitization event (Hu et al., 2020b; Jiang et al., 2022b). While D2 dolomites occur as ctenoid cements in the Longwangmiao Formation, indicating that they were early diagenetic products as well (Liu et al., 2021). D2 dolomite in both formations could have been related to the elevated Mg/Ca ratio either due to abundant sulfate precipitation by evaporation or

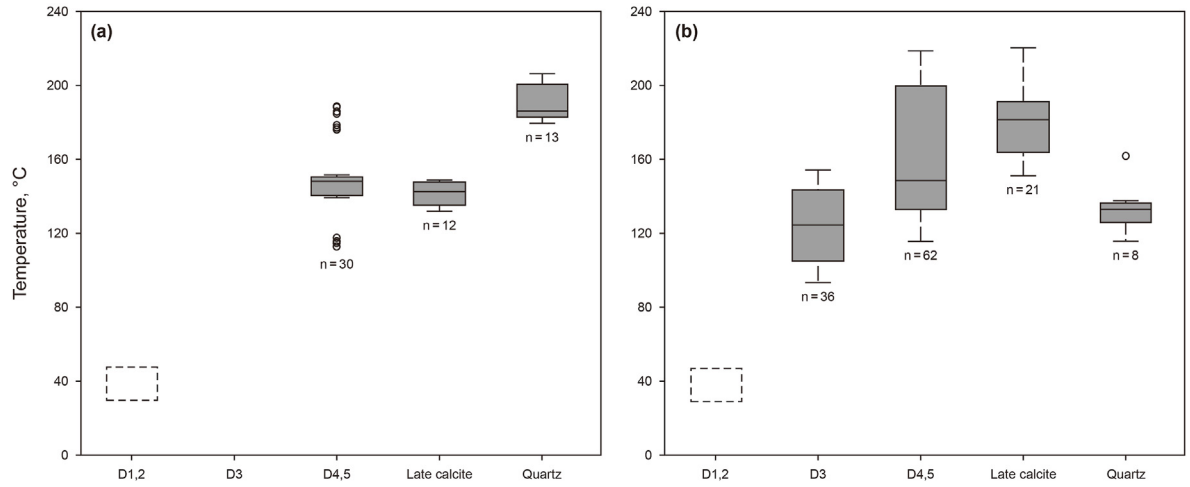

Fig. 7. Compiled homogenization temperatures for late diagenetic minerals in the Longwangmiao Formation (a) and Dengying Formation (b), the dash lined rectangle represents the diagenetic temperatures for reflux dolomitization measured from clumped isotopes, modified after Jiang et al. (2022b); Liu et al. (2021). Data sources of temperatures are listed in the supplementary data file.

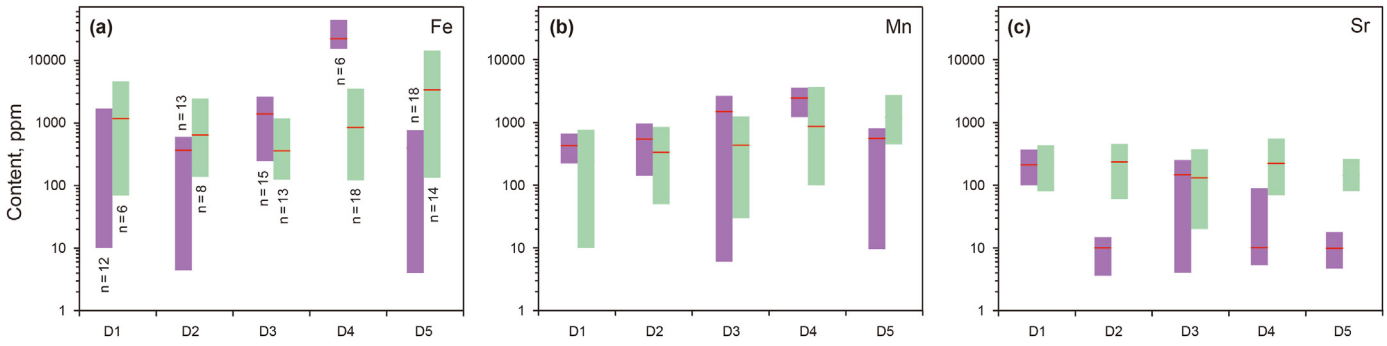

Fig. 8. Elements content in various type of dolomites in the Longwangmiao Formation (purple bar) and Dengying Formation (green bar). (a) Fe element; (b) Mn element; (c) Sr element. Red line with each bar stands for the mean value.

Table 1
Trace element contents and Sr isotopic compositions of various types of carbonate minerals in the Longwangmiao Formation and Dengying Formation.

Longwangmiao Formation	Mineral	FeO/average, ppm	MnO/average, ppm	SrO/average, ppm	$^{87}Sr/^{86}Sr$	Homogenization Temperature, °C
Dolomite Matrix	D1	10–1880/1136[a]	210–690/434[a]	100–390/210[a]	0.7095 to 0.7116[b]	<50[b]
Interparticle dolomite cement	D2	2250–2670/2443[a]	190–290/246[a]	260–370/300[a]	0.7094[b]	<50[b]
Isopachous dolomite cement	D2	10–670/391[a]	140–970/528[a]	7–15/10[a]	0.7103 to 0.7108[b]	<50[b]
Medium poikilitic dolomite cement	D3	250–2720/1362[a]	10–2860/1420[a]	10–280/173[a]	0.7093 to 0.7107[b]	100 to 114[b]
Medium to coarse dolomite cement	D4	17,680–46,900/22,424[a]	1290–3510/2512[a]	5–20/10[a]	0.7128[b]	138 to 142[b]
Coarse rhombic dolomite cement	D5	10–790/415[a]	10–880/576[a]	8–20/10[a]	0.7098 to 0.7100[b]	147 to 190[b]
Late calcite cements	Cal	nd	nd	nd	nd	140 to 160[b]

Dengying Formation	Mineral	FeO/average, ppm	MnO/average, ppm	SrO/average, ppm	$^{87}Sr/^{86}Sr$	Homogenization Temperature, °C
Dolomite Matrix	D1	70–4720/1098[c]	10–740/257[c]	80–410/214[c]	0.7084 to 0.7092[c]	<50[c]
Fibrous dolomite cements	D2	140–2450/691[c]	50–810/336[c]	60–450/234[c]	0.7089 and 0.7090[c]	<50[c]
Bladed dolomite cements	D3	230–1110/386[c]	30–1090/435[c]	20–390/187[c]	0.7089 and 0.7092[c]	90 to 120[c]
Medium- to coarse-crystalline dolomite cements	D4	110–3720/860[c]	100–2760/848[c]	70–550/216[c]	0.7093 and 0.7095[c]	120 to 160[c]
Saddle dolomite	D5	140–14,810/3449[c]	450–2890/1272[c]	80–270/155[c]	0.7101 to 0.7128[c]	160 to 220[c]
Late calcite cements	Cal	nd	nd	nd	nd	150 to 220[c]

Note.
[a] Marked data cited from Liu et al. (2020).
[b] Marked data cited from Liu et al. (2021).
[c] Marked data cited from Hu et al. (2020a,b).

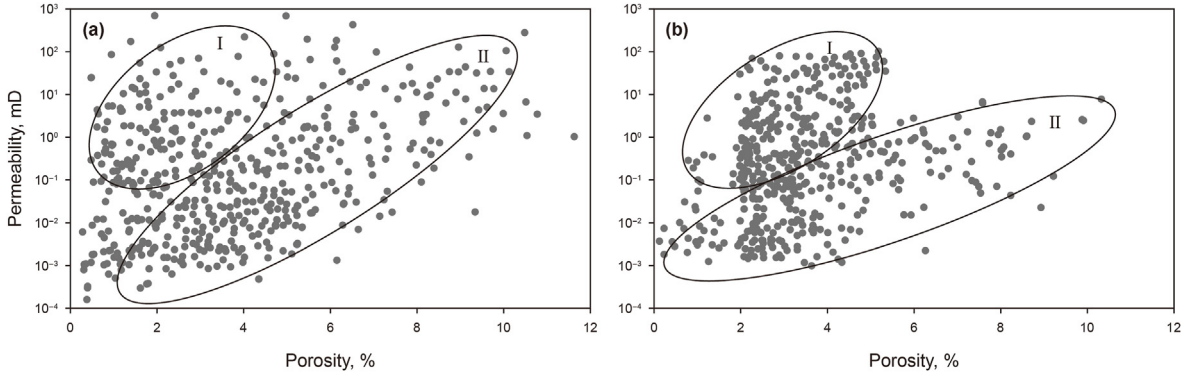

Fig. 9. Compiled cross plot of porosity and permeability data for typical dolostone reservoirs in the Longwangmiao Formation (a) and Dengying Formation (b). Two groups of distribution pattern (I and II) are present in both formations.

inherited from the original seawater (vS Hood et al., 2011; Wood et al., 2017; Jiang et al., 2022b). Recrystallization by evaporated seawater may have persisted throughout the shallow burial diagenetic realm, allowing the entire carbonate platform was completely dolomitized (Jiang et al., 2022b). The wide occurrence of meteoric diagenesis due to epigenic karstification has been documented in both formations, as supported by petrophysics data and porosity, petrology of diagenetic carbonates, carbon and oxygen, as well as trace elements (Jin et al., 2014; Yang et al., 2016; Zhou et al., 2020; Liu et al., 2021; Xu et al., 2022; Hu et al., 2023). Meteoric diagenesis may have slightly postdated matrix dolomitization event in the Dengying Formation (Hu et al., 2020b; Jiang et al., 2022b; Xu et al., 2022), whereas it likely preceded the matrix dolomitization event in the Longwangmiao Formation (Yang

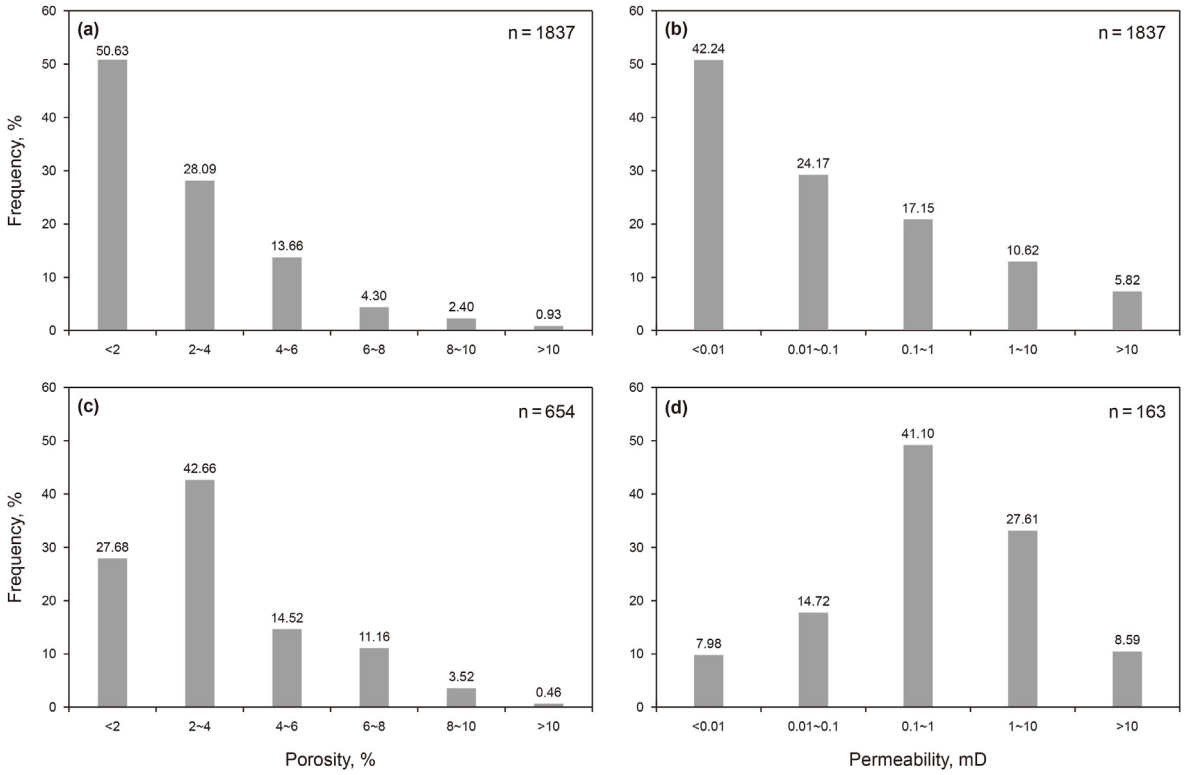

Fig. 10. Histograms comparing the distribution characteristics of porosity and permeability in the Longwangmiao Formation (a, c) and Dengying Formation (b, d).

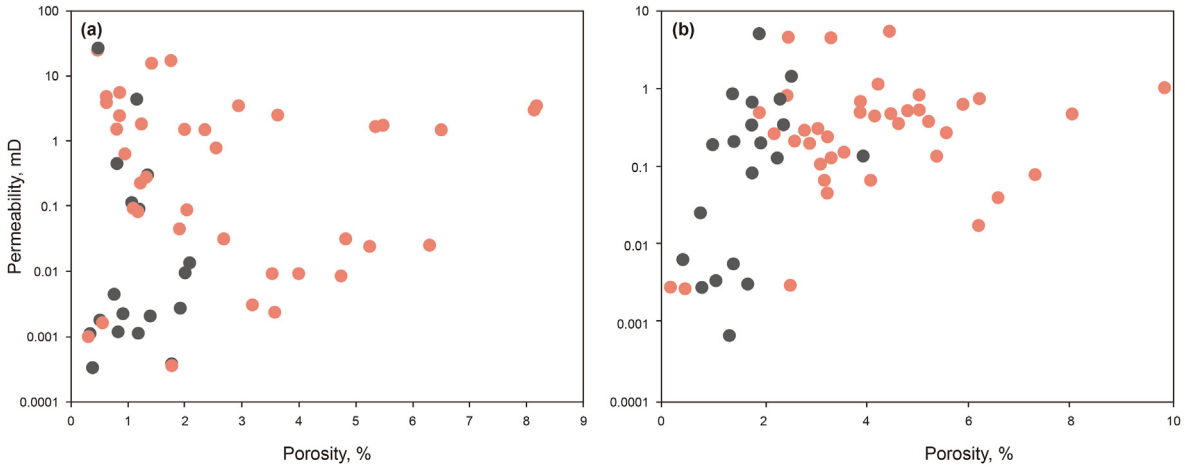

Fig. 11. The coupling relationship between tectonic and carbonate reservoir quality. (a) High reservoir quality is associated with open fractures displaying abundant dissolution porosity from the Longwangmiao Formation; (b) high reservoir quality present at places where experienced massive hydrothermal alternations from the Dengying Formation. Red and black filled circles represent the data obtained from fracture-related reservoir and matrix dolostone, respectively.

et al., 2016; Liu et al., 2021). The markedly elevated $^{87}Sr/^{86}Sr$ ratios in D1 and subsequent D2 and D3 dolomites in the Longwangmiao Formation (Fig. 13f) was likely related to the increased influx of ^{87}Sr-riched silicate from the surrounding paleo-terrestrial highlands by meteoric leaching (Yang et al., 2016; Liu et al., 2021; Hu et al., 2023). The slightly negative shifts of $\delta^{13}C$ and $\delta^{18}O$ along with increased Fe and Al contents in host rocks further support the occurrence of epigenic karstification in both formation (Liu et al., 2021; Hu et al., 2023). Note that the exposure time for the Longwangmiao Formation in the northwest part of basin has lasted about 120 Ma from the middle Silurian to Permian (Jin et al., 2014; Yang et al., 2016), resulting in more intensive meteoric alternation on carbonates geochemistry data, such as $\delta^{18}O$ and $^{87}Sr/^{86}Sr$, compared with those of the Dengying Formation (Fig. 13).

The precipitation of most dolomite cements (D3) seems to inherit the element concentrations, $\delta^{13}C$ and $^{87}Sr/^{86}Sr$ signals from their matrix dolomite (D1) (Figs. 5–7 and 13). Together with the marked lower $\delta^{18}O$ (Fig. 7b and 13c, d) and younger U-Pb ages (middle Cambrian to middle Ordovician; Fig. 12) compared with the D1 and D2 dolomites, suggesting that they were most plausibly related to solution-compaction during shallow burial conditions (Jiang et al., 2018c; Xu et al., 2022; Li et al., 2023). Subsequently, the initial major oil charging event in both formations may have occurred during the late stage of Caledonian uplift (Fig. 12) (Liu

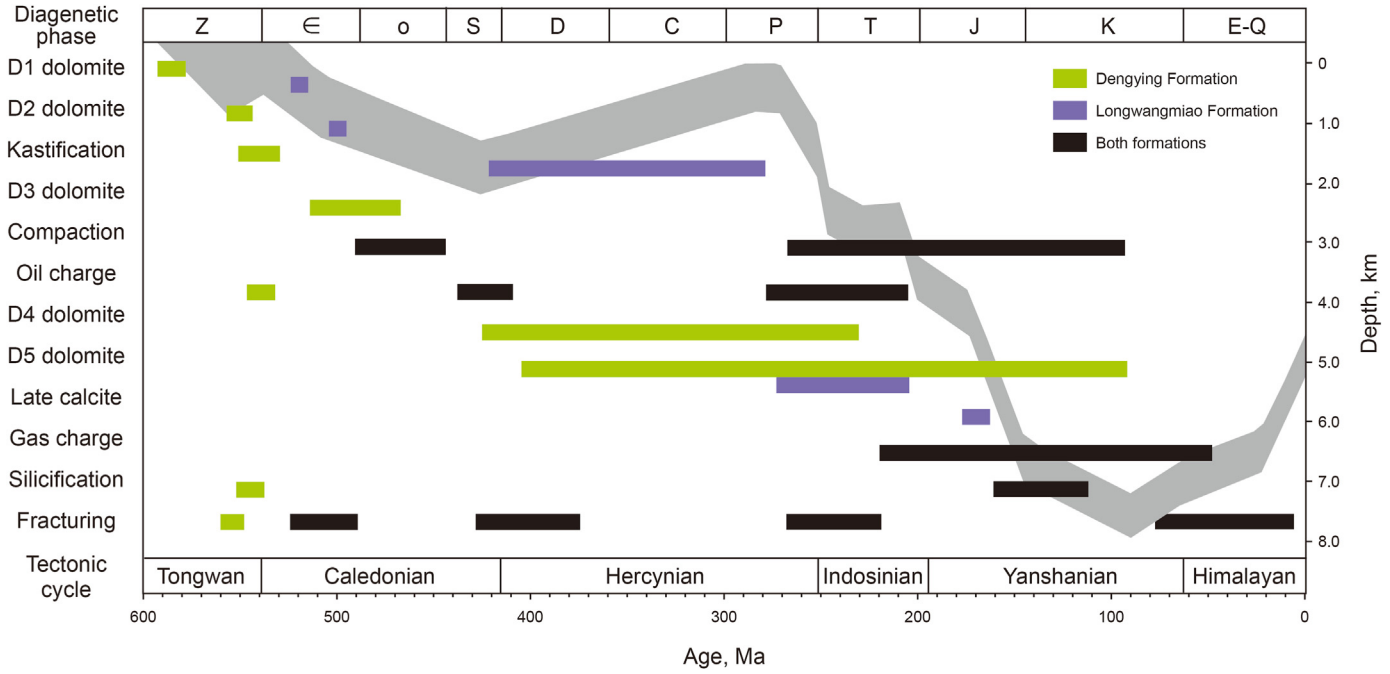

Fig. 12. The comparation of diagenetic sequence model along with burial evolution curve (in gray) in the Dengying Formation (green bar) and Longwangmiao Formation (purple bar), while black bar stands for diagenetic event occurred in both formations. Age constrains for each diagenetic phase refer to age model present in Fig. 2.

et al., 2021; Shen et al., 2021; Xu et al., 2022; Li et al., 2023). The following diagenesis was dominated by D4 and D5 dolomites precipitation occurred at intermediate to deep burial diagenetic realm mainly between ≃ 400 Ma and 100 Ma (Fig. 12). This long-lasting diagenetic phase was likely coupled with multiphase hydrothermal activities in both formations, resulted in the generation of hydrothermal mineral assemblages, consisting mainly of dolomite, calcite, fluorite, bitumen, and quartz (Hu et al., 2020b; Liu et al., 2021; Su et al., 2022; Xu et al., 2022; Gu et al., 2023). The marked lighter $\delta^{18}O$ values (Fig. 13) along with elevated temperatures (Fig. 7) confirming that some D4 and D5 dolomites were likely precipitated from hydrothermal fluids (Su et al., 2022; Gu et al., 2023; Li et al., 2023). Additionally, the markedly elevated $^{87}Sr/^{86}Sr$ ratios in hydrothermal minerals, such as saddle dolomites (D5), in both formations (Fig. 13e, f), supporting an external, deep basinal sourced ^{87}Sr-riched hydrothermal fluids likely related to faults and fractures caused by tectonics (Figs. 2 and 12). This assertation agrees well with elevated $^{87}Sr/^{86}Sr$ ratios measured from hydrothermal dolomites within or near the deep-rooted fractures (Fig. 14). Notably, the second major oil generation and charging occurred between the middle Permian and late Triassic, followed by gas generation due to thermal cracking of oil throughout the entire Mesozoic (Su et al., 2020). The above hydrocarbon generation events mostly overlapped with the rapid burial stage during the Indosinian-Yanshanian tectonic period (Fig. 12).

5.2. Diagenetic effects on reservoir formation

The distribution range and pattern of porosity and permeability of carbonate reservoirs are nearly identical in both formations (Fig. 9), despite their differential compositions, textures, initial porosity, and diagenetic alternations. However, several diagenetic processes could have affected these reservoir qualities, such as the generation of intercrystalline pores by matrix dolomtization (Saller et al., 2014; Jiang, 2022), creation of vuggy and dissolution-enlarge pores by meteoric diagenesis and hydrothermal alternation and thermochemical sulfate reduction (Hu et al., 2020b; Liu et al., 2021). Better reservoir quality found in the Dengying Formation is attributed mainly to more extensive fracturing (Fig. 14) and hydrothermal fluid alterations (Fig. 7) than those of the Longwangmiao Formation. These tectonic-related activities may have markedly increased the permeability rather than porosity of these reservoirs (Fig. 10) (Hu et al., 2020b; Wei et al., 2022; Xu et al., 2022). The observation that markedly increased permeability which is tightly linked to fractures within well intervals in both formations (Fig. 11), supporting the crucial role of tectonics on the development of these reservoirs.

The primary porosity of these reservoirs was closely related to sedimentary facies, agreeing with many previous investigations that the best reservoirs of both formations are predominantly preserved in high-energy facies (Yang et al., 2016; Zhou et al., 2016; Hu et al., 2020b; Liu et al., 2021). Meteoric water influx by epigenic karstification may have shortly postdated the matrix (reflux) dolomitization event (Xu et al., 2022; Hu et al., 2023). However, despite the much longer exposure time (≃ 120 Ma) and thus the more intensive epigenic karstification in the Longwangmiao Formation, it displays poorer reservoir quality than the Dengying Formation (Figs. 9 and 10). This boosts the case that epigenic karstification likely has only played a subsidiary role on superior reservoir quality development in these carbonates (Liu et al., 2021). A possible explanation is that a much lower dissolution rate for dolomite compared with calcite by meteoric water leaching. Alternatively, most of secondary porosity produced by epigenic karstification may have been destroyed by burial compaction and mineral cementation.

Higher porosity preserved in dolostones compared with their contemporaneous limestones counterpart has been commonly attributed to early dolomitization, which has allowed the preservation of porosity against carbonate cementation through burial compaction (Jiang et al., 2018c). Therefore, matrix dolomitization is an essential prerequisite for the formation of superior reservoir in

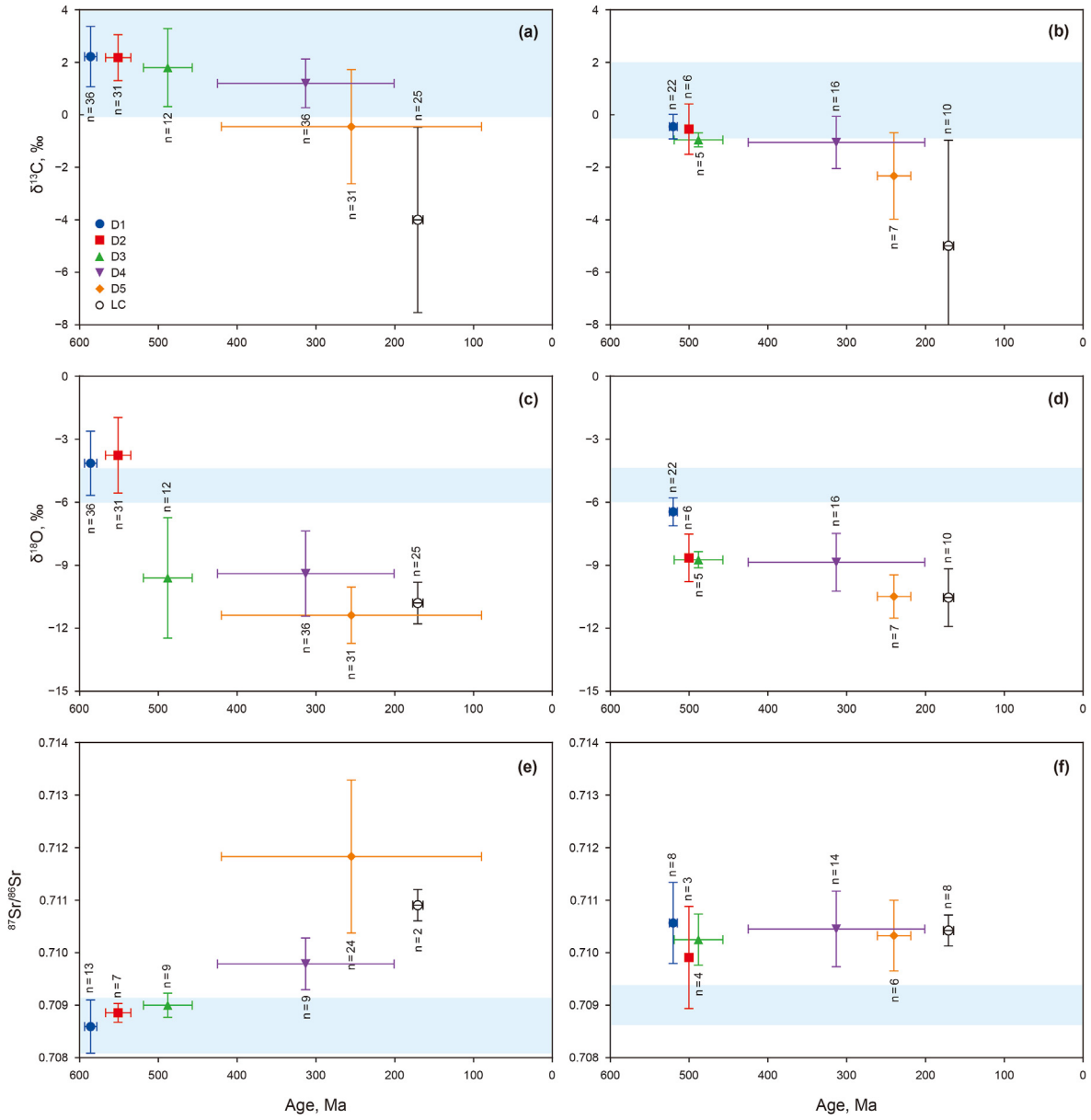

Fig. 13. Diagenetic evolution of $\delta^{13}C$, $\delta^{18}O$, and $^{87}Sr/^{86}Sr$ isotopes in the Dengying Formation (a, c, e) and Longwangmiao Formation (b, d, f), coupled with the established age model in Fig. 2b. Blue bar in each sub-figure represents coeval seawater isotopic range modified after Li et al. (2023).

the Dengying Formation and Longwangmiao Formation (Hu et al., 2020b; Liu et al., 2021; Xu et al., 2022; Li et al., 2023). Additionally, the relative early oil emplacement, which started at ≃450 Ma with burial depths of < 2000 m (Fig. 12), in these reservoirs may have inhibited dolomite growth in the residue pore spaces and further preserved their primary porosity from losing against burial compaction (Jiang et al., 2018c).

Notably, the wide occurrence of hydrothermal activity, as revealed by abundant hydrothermal mineral assembles, such as saddle dolomite, fluorite, quartz, and calcite, within fractures and faults in both formations (Fig. 14) (Hu et al., 2020b; Liu et al., 2021; Jiang et al., 2022b; Xu et al., 2022), has been tightly linked to the Indosinian and subsequent Yanshanian tectonic movement (Fig. 12) (Liu et al., 2021; Xu et al., 2022). The reservoir quality could be either increased by fracturing, thermochemical sulfate reduction, or decreased by hydrothermal minerals and bitumen filling, yielding a near unchanged net porosity during this hydrothermal event (Liu et al., 2021; Xu et al., 2022). Instead, fractures and faults may have enhanced reservoir quality by the markedly increased permeability (Figs. 9 and 10). This may be crucial in affecting the reservoir quality differentially in both formations, depending on the intensity of hydrothermal alternations linked to tectonics (Figs. 7 and 14).

5.3. Implications for the origin of deep burial carbonate reservoirs

This new contribution highlights that the combination of petrology and geochemistry and petrophysics analysis, coupled with data compilation, is an effective toolkit to decipher the diagenetic evolution and reservoir development model for deep burial carbonates (Qing and Mountjoy, 1994; Palmer, 1995; Jiang et al., 2018a, 2018b, 2018c). The exploration of petroleum and geothermal energy resources in carbonates of Cambrian and pre-Cambrian ages, which mainly consists of dolostone, has been

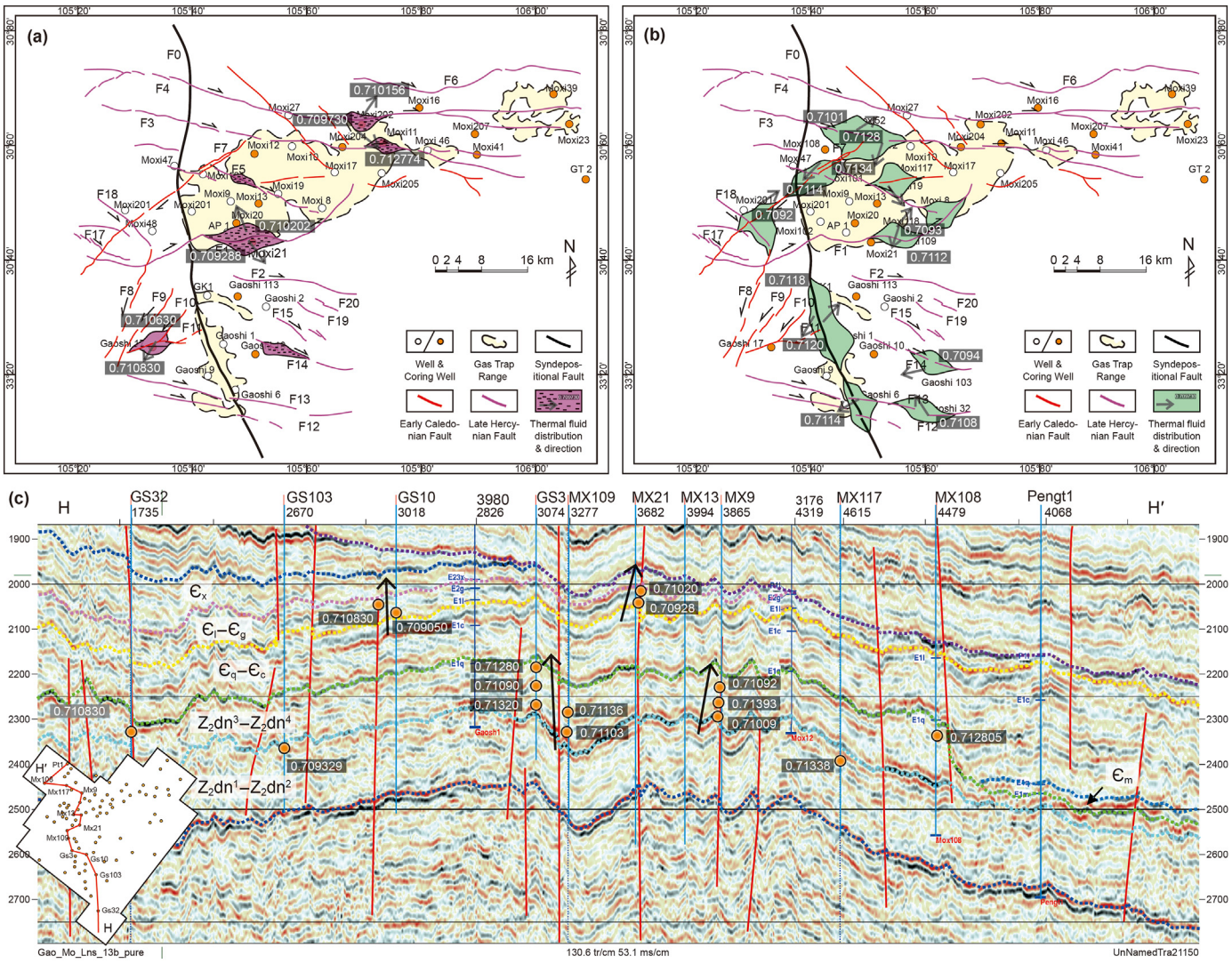

Fig. 14. Geological map showing the main hydrothermal activity in the Longwangmiao Formation (a) and Dengying Formation (b), the direction of hydrothermal fluid is suggested by decreased $^{87}Sr/^{86}Sr$ trend. (c) A North-South direction seismic profile showing hydrothermal activity along faults.

placed increasing importance in China (Wei et al., 2022). The mechanisms for reservoir formation in deeply buried carbonates therefore are crucial in the efficiency exploration of these petroleum resources. This study strengthens the case that superior carbonate reservoir quality is closely linked to high-energy facies superimposed with several key profitable diagenetic alternations, such as dolomitization, meteoric, fracturing and hydrothermal fluids. This basic understanding concurs with the general exploration experiences from most of Phanerozoic dolostone reservoirs as well (Grotzinger and Al-Rawahi, 2014; Saller et al., 2014; Jiang et al., 2018b, 2018c).

Carbonate reservoirs from both of the Longwangmiao Formation and Dengying Formation may have been completely dolomitized at the very early diagenetic stage (Jiang et al., 2022b), allowing effective preservation of primary pore system from progressive losing by burial compaction. Meteoric leaching by epigenic karstification may have only played a subsidiary role in the development of these reservoirs, despite its wide occurrence in those reservoirs (see detailed discussion in the above section). Crucially, our new contribution provides evidence for a tight coupling relationship between reservoir development and the intensity of fracture and hydrothermal fluid activities caused by tectonics. Mechanisms for carbonate dissolution related to tectonics include fluids mixing, cooling of hydrothermal fluids, hypogenic karstification, thermochemical and bacterial sulfate reductions (Mazzullo and Harris, 1991; Hill, 1995; Loucks, 1999; Heydari, 2000; Jiang et al., 2018a, 2018b, 2018c). However, reservoir quality enhancement likely have been neutralized by the precipitation of hydrothermal minerals during the hydrothermal event. Instead, reservoir quality enhancement by tectonic is predominantly attributed to markedly increased permeability rather than porosity (Figs. 9 and 10). Hence, good reservoirs are preferentially preserved at or near to the faults and fractures, which would have practical implications for reservoir prediction during future exploration of deep to ultra-deep carbonates in the Sichuan Basin and Tarim Basin in China (Wei et al., 2022; Jiang et al., 2023).

6. Conclusions

Dolostone gas reservoirs of the Lower Cambrian Longwangmiao Formation and Upper Ediacaran Dengying Formation from the Central Sichuan Basin, China, were selected for comprehensive petrology and geochemistry data analyzes in this study. Specifically, we compiled a wide range of geochemistry and petrophysics data,

coupled with newly analyzed petrology and geochemistry data, aiming to build a synthesized diagenetic evolution model and establish the causal relationships between several profitable diagenesis and their specific roles on reservoir development. Collectively, five similar dolomite phases, as inferred by different occurrence of dolomite (D1–5), were identified in both formations. D1 and D2 dolomites were likely linked to reflux of evaporated seawater with markedly high Mg/Ca ratio. The elevated $^{87}Sr/^{86}Sr$ in some D1 dolomites implied the existence of paleo highlands near the carbonate platform during deposition. Early matrix dolomitization was contributed to the preservation of major primary porosity against burial compaction. Although epigenic karstification had widely occurred in both formations, it may have not apparently improved the reservoir quality due to: i) low dissolution rate by leaching of dolomite relative to calcite, and/or ii) porosity decreasing due to carbonate cementation resulted by burial compaction. The widespread hydrothermal activities may have allowed the enhancement of reservoir quality mostly by increasing of permeability rather than porosity. This study highlights the crucial role of tectonic on the development of superior dolostone reservoirs in the Longwangmiao Formation and Dengying Formation, a typical Ediacaran-Cambrian transition profile in the Sichuan Basin in China. The outcomes of this study allows more explicit reservoir prediction direction in the deep to ultra-deep buried carbonates in the Sichuan Basin, as well as other sedimentary basin analogues in China, such as the Tarim Basin, Ordos Basin, and many sub-basins from the North China Craton.

Declaration of interest statement

This submission has not been published previously including in the form of an abstract, a published lecture or academic thesis. It is also not under consideration for publication elsewhere. This publication is approved by all authors and tacitly or explicitly by the responsible authorities where the work was carried out, and that, if accepted, it will not be published elsewhere in the same form, in English or in any other language, including electronically without the written consent of the copyright-holder.

Acknowledgments

This paper was financially supported by grants from the National Natural Science Foundation of China (41972149, 41890843).

Appendix A. Supplementary data

Supplementary data to this article can be found online at https://doi.org/10.1016/j.petsci.2023.09.025.

References

Bergmann, K.D., Al Balushi, S.A., Mackey, T.J., Grotzinger, J.P., Eiler, J.M., 2018. A 600-million-year carbonate clumped-isotope record from the Sultanate of Oman. J. Sediment. Res. 88, 960–979. https://doi.org/10.2110/jsr.2018.51.

Davies, G.R., Smith Jr., L.B., 2006. Structurally controlled hydrothermal dolomite reservoir facies: an overview. AAPG Bull. 90, 1641–1690. https://doi.org/10.1306/05220605164.

Ehrenberg, S.N., Walderhaug, O., Bjørlykke, K., 2012. Carbonate porosity creation by mesogenetic dissolution: reality or illusion? AAPG Bull. 96, 217–233. https://doi.org/10.1306/05031110187.

Feng, M.Y., Wu, P.C., Qiang, Z.T., Liu, X.H., Duan, Y., Xia, M.L., 2017. Hydrothermal dolomite reservoir in the precambrian Dengying Formation of central Sichuan Basin, southwestern China. Mar. Petrol. Geol. 82, 206–219. https://doi.org/10.1016/j.marpetgeo.2017.02.008.

Fu, Q.L., Hu, S.Y., Xu, Z.H., Zhao, W.Z., Shi, S.Y., Zeng, H.L., 2020. Depositional and diagenetic controls on deeply buried Cambrian carbonate reservoirs: Longwangmiao Formation in the Moxi-Gaoshiti area, Sichuan Basin, southwestern China. Mar. Petrol. Geol. 117, 104318. https://doi.org/10.1016/j.marpetgeo.2020.104318.

Grotzinger, J., Al-Rawahi, Z., 2014. Depositional facies and platform architecture of microbialite-dominated carbonate reservoirs, Ediacaran-Cambrian Ara Group, Sultanate of OmanMicrobialite Reservoirs in Oman. AAPG Bull. 98, 1453–1494. https://doi.org/10.1306/02271412063.

Gu, Y.F., Wang, Z.L., Yang, C.C., Luo, M.S., Jiang, Y.Q., Luo, X.R., Zhou, L., Wang, H.J., 2023. Effects of diagenesis on quality of dengying formation deep dolomite reservoir, Central Sichuan Basin, China: insights from petrology, geochemistry and in situ U-Pb dating. Front. Earth Sci. 10, 1041164. https://doi.org/10.3389/feart.2022.1041164.

Halverson, G.P., Dudás, F.Ö., Maloof, A.C., Bowring, S.A., 2007. Evolution of the $^{87}Sr/^{86}Sr$ composition of Neoproterozoic seawater. Palaeogeogr. Palaeoclimatol. Palaeoecol. 256, 103–129. https://doi.org/10.1016/j.palaeo.2007.02.028.

Hao, F., Zhang, X.F., Wang, C.W., Li, P.P., Guo, T.L., Zou, H.Y., Zhu, Y.M., Liu, J.Z., Cai, Z.X., 2015. The fate of CO_2 derived from thermochemical sulfate reduction (TSR) and effect of TSR on carbonate porosity and permeability, Sichuan Basin, China. Earth Sci. Rev. 141, 154–177. https://doi.org/10.1016/j.earscirev.2014.12.001.

Heydari, E., 2000. Porosity loss, fluid flow, and mass transfer in limestone reservoirs: application to the Upper Jurassic Smackover Formation, Mississippi. AAPG Bull. 84, 100–118. https://doi.org/10.1306/C9EBCD79-1735-11D7-8645000102C1865D.

Hill, C.A., 1995. H_2S-related porosity and sulfuric acid oil-field karst. In: Budd, D.A., Saller, A.H., Harris, P.M. (Eds.), Unconformities and Porosity in Carbonate Strata, vol. 63. AAPG Mem, pp. 301–306.

Hu, Y.J., Cai, C.F., Liu, D.W., Pederson, C.L., Jiang, L., Shen, A.J., Immenhauser, A., 2020a. Formation, diagenesis and palaeoenvironmental significance of upper Ediacaran fibrous dolomite cements. Sedimentology 67, 1161–1187. https://doi.org/10.1111/sed.12683.

Hu, Y.J., Cai, C.F., Pederson, C.L., Liu, D.W., Jiang, L., He, X.Y., Shi, S.Y., Immenhauser, A., 2020b. Dolomitization history and porosity evolution of a giant, deeply buried Ediacaran gas field (Sichuan Basin, China). Precambrian Res. 338, 105595. https://doi.org/10.1016/j.precamres.2020.105595.

Hu, Y.J., Cai, C.F., Liu, D.W., Peng, Y.Y., Wei, T.Y., Jiang, Z.W., Ma, R.T., Jiang, L., 2021. Distinguishing microbial from thermochemical sulfate reduction from the upper Ediacaran in South China. Chem. Geol. 583, 120482. https://doi.org/10.1016/j.chemgeo.2021.120482.

Hu, Y.J., Cai, C.F., Li, Y., Liu, D.W., Wei, T.Y., Wang, D.W., Jiang, L., Ma, R.T., Shi, S.Y., Immenhauser, A., 2023. Sedimentary and diagenetic archive of a deeply buried, upper Ediacaran microbialite reservoir, southwestern China. AAPG Bull. 107, 387–412. https://doi.org/10.1306/08232221122.

Jiang, L., 2022. Diagenesis of the san andres Formation in the seminole unit in central basin platform, western Texas. AAPG Bull. 106, 267–287. https://doi.org/10.1306/08092118042.

Jiang, L., Worden, R.H., Yang, C.B., 2018a. Thermochemical sulphate reduction can improve carbonate petroleum reservoir quality. Geochem. Cosmochim. Acta 223, 127–140. https://doi.org/10.1016/j.gca.2017.11.032.

Jiang, L., Worden, R.H., Cai, C.F., Shen, A.J., Crowley, S.F., 2018b. Diagenesis of an evaporite-related carbonate reservoir in deeply buried Cambrian strata, Tarim Basin, Northwest China. AAPG Bull. 102, 77–102. https://doi.org/10.1306/0328171608517048.

Jiang, L., Worden, R.H., Cai, C.F., Shen, A.J., He, X.Y., Pan, L.Y., 2018c. Contrasting diagenetic evolution patterns of platform margin limestones and dolostones in the Lower Triassic Feixianguan Formation, Sichuan Basin, China. Mar. Petrol. Geol. 92, 332–351. https://doi.org/10.1016/j.marpetgeo.2017.10.029.

Jiang, L., Zhao, M.Y., Shen, A.J., Huang, L.L., Chen, D.Z., Cai, C.F., 2022a. Pulses of atmosphere oxygenation during the Cambrian radiation of animals. Earth Planet Sci. Lett. 590, 117565. https://doi.org/10.1016/j.epsl.2022.117565.

Jiang, L., Shen, A.J., Wang, Z.C., Hu, A.P., Wang, Y.S., Luo, X.Y., Liang, F., Azmy, K., Pan, L.Y., 2022b. U-Pb geochronology and clumped isotope thermometry study of Neoproterozoic dolomites from China. Sedimentology 69, 2925–2945. https://doi.org/10.1111/sed.13026.

Jiang, L., Shen, A.J., Qiao, Z.F., Hu, A.P., Xu, Z.H., Zhang, H., Wan, B., Cai, C.F., 2023. Hypogenic karstic cavities formed by tectonic-driven fluid mixing in the Ordovician Carbonates from the Tarim Basin, NW China. AAPG Bull. https://doi.org/10.1306/08022321011.

Jin, M., Zeng, W., Tan, X.C., Li, L., Li, Z.Y., Luo, B., Zhang, J.L., Liu, J.W., 2014. Characteristics and controlling factors of beach-controlled karst reservoirs in cambrian Longwangmiao Formation, moxi-gaoshiti area, Sichuan Basin, NW China. Petrol. Explor. Dev. 41, 712–723. https://doi.org/10.1016/S1876-3804(14)60085-9.

Kochnev, B., Pokrovsky, B., Kuznetsov, A., Marusin, V., 2018. C and Sr isotope chemostratigraphy of Vendian-Lower Cambrian carbonate sequences in the central Siberian Platform. Russ. Geol. Geophys. 59, 585–605. https://doi.org/10.1016/j.rgg.2018.05.001.

Li, C.R., Pang, X.Q., Ma, X.H., Wang, E.Z., Hu, T., Wu, Z.Y., 2021. Hydrocarbon generation and expulsion characteristics of the Lower Cambrian Qiongzhusi shale in the Sichuan Basin, Central China: implications for conventional and unconventional natural gas resource potential. J. Petrol. Sci. Eng. 204, 108610. https://doi.org/10.1016/j.petrol.2021.108610.

Li, K.K., Gong, B.R., Zhang, X.H., Jiang, H., Fan, J.J., Tan, Y.N., 2023. A comparison of hydrothermal events and petroleum migration between Ediacaran and lower Cambrian carbonates, Central Sichuan Basin. Mar. Petrol. Geol. 150, 106130. https://doi.org/10.1016/j.marpetgeo.2023.106130.

Liu, D.W., Cai, C.F., Hu, Y.J., Jiang, L., Peng, Y.Y., Yu, R., Qin, Q., 2020. Multi-stage dolomitization process of deep burial dolostones and its influence on pore

evolution: a case study of Longwangmiao formation in the Lower Cambrian of central Sichuan Basin. J. China Inst. Min. Technol. 49, 1150–1165 (in Chinese).
Liu, D.W., Cai, C.F., Hu, Y.J., Peng, Y.Y., Jiang, L., 2021. Multistage dolomitization and formation of ultra-deep lower cambrian Longwangmiao Formation reservoir in central Sichuan Basin, China. Mar. Petrol. Geol. 123, 104752. https://doi.org/10.1016/j.marpetgeo.2020.104752.
Liu, Q.Y., Zhu, D.Y., Jin, Z.J., Liu, C.Y., Zhang, D.W., He, Z.L., 2016. Coupled alteration of hydrothermal fluids and thermal sulfate reduction (TSR) in ancient dolomite reservoirs-An example from Sinian Dengying Formation in Sichuan Basin, southern China. Precambrian Res. 285, 39–57. https://doi.org/10.1016/j.precamres.2016.09.006.
Liu, W., Qiu, N.S., Xu, Q.C., Chang, J., 2018. The quantitative evaluation of the pressurization caused by hydrocarbon generation in the Cambrian Qiongzhusi Formation of the Gaoshiti-Moxi area, Sichuan Basin. Petrol. Sci. Bull. 3, 262–271 (in Chinese).
Loucks, R.G., 1999. Paleocave carbonate reservoirs: origins, burial-depth modifications, spatial complexity, and reservoir implications. AAPG Bull. 83, 1795–1834. https://doi.org/10.1306/E4FD426F-1732-11D7-8645000102C1865D.
Luo, B., Yang, Y.M., Luo, W.J., Wen, L., Wang, W.Z., Chen, K., 2017. Controlling factors of Dengying Formation reservoirs in the central Sichuan paleo-uplift. Petrol. Res. 2, 54–63. https://doi.org/10.1016/j.ptlrs.2017.06.001.
Mazzullo, S., Harris, P., 1991. An overview of dissolution porosity development in the deep-burial environment, with examples from carbonate reservoirs in the Permian Basin. In: Candelaria, M. (Ed.), Permian Basin Plays-Tomorrow's Technology Today. West Texas Geological Society, Midland, TX, 91–89.
Montañez, I.P., Osleger, D.A., Banner, J.L., Mack, L.E., Musgrove, M., 2000. Evolution of the Sr and C isotope composition of Cambrian oceans. GSA oday 10, 1–7.
Palmer, A.N., 1995. Geochemical models for the origin of macroscopic solution porosity in carbonate rocks. In: Budd, D.A., Saller, A.H., Harris, P.M. (Eds.), Unconformities and Porosity in Carbonate Strata, vol. 63. AAPG Mem, pp. 77–101.
Pokrovsky, B.G., Mavromatis, V., Pokrovsky, O.S., 2011. Co-variation of Mg and C isotopes in late Precambrian carbonates of the Siberian Platform: a new tool for tracing the change in weathering regime? Chem. Geol. 290, 67–74. https://doi.org/10.1016/j.chemgeo.2011.08.015.
Qiao, Z.F., Dong, J.H., Yu, Z., Li, W.Z., Wang, X.F., Jiang, L., Qing, H.R., 2022. Diagenesis and reservoir evolution model of the ediacaran dengying Formation in the Sichuan Basin: evidence from laser ablation U-Pb dating and in situ isotope analysis. Minerals 12, 1372. https://doi.org/10.3390/min12111372.
Qing, H.R., Mountjoy, E.W., 1994. Origin of dissolution vugs, caverns, and breccias in the Middle Devonian Presqu'ile barrier, host of Pine Point Mississippi valley-type deposits. Econ. Geol. 89, 858–876. https://doi.org/10.2113/gsecongeo.89.4.858.
Ren, Y., Zhong, D.K., Gao, C.L., Sun, H.T., Peng, H., Zheng, X.W., Qiu, C., 2019. Origin of dolomite of the lower cambrian Longwangmiao Formation, eastern Sichuan Basin, China. Carbonate. Evaporite 34, 471–490. https://doi.org/10.1007/s13146-017-0409-7.
Ren, Y., Zhong, D.K., Cao, C.L., Yang, Q.Q., Xie, R., Jia, L.B., Jiang, Y.J.F., Zhong, N.C., 2017. Dolomite geochemistry of the cambrian Longwangmiao Formation, eastern Sichuan Basin: implication for dolomitization and reservoir prediction. Petrol. Res. 2, 64–76. https://doi.org/10.1016/j.ptlrs.2017.06.002.
Saller, A.H., Henderson, N., 1998. Distribution of porosity and permeability in platform dolomites: insight from the Permian of west Texas. AAPG Bull. 82, 1528–1550. https://doi.org/10.1306/1D9BCB01-172D-11D7-8645000102C1865D.
Saller, A.H., Pollitt, D., Dickson, J., 2014. Diagenesis and porosity development in the first eocene reservoir at the giant wafra field, partitioned zone, Saudi arabia and KuwaitDiagenesis of the first eocene, wafra field. AAPG Bull. 98, 1185–1212. https://doi.org/10.1306/12021313040.
Shen, A.J., Chen, Y.N., Pan, L.Y., Wang, L., She, M., 2018. Facies and porosity origin of reservoirs: case studies from the Cambrian Longwangmiao Formation of Sichuan Basin, China, and their implications on reservoir prediction. J. Nat. Gas Geos. 3, 37–49. https://doi.org/10.1016/j.jnggs.2018.03.003.
Shen, A.J., Luo, X.Y., Hu, A.P., Qiao, Z.F., Zhang, J., 2022. Dolomitization evolution and its effects on hydrocarbon reservoir formation from penecontemporaneous to deep burial environment. Petrol. Explor. Dev. 49, 731–743. https://doi.org/10.1016/S1876-3804(22)60306-9.
Shen, A.J., Zhao, W.Z., Hu, A.P., Wang, H., Liang, F., Wang, Y.S., 2021. The dating and temperature measurement technologies for carbonate minerals and their application in hydrocarbon accumulation research in the paleo-uplift in central Sichuan Basin, SW China. Petrol. Explor. Dev. 48, 555–568. https://doi.org/10.1016/S1876-3804(21)60045-9.
Shi, C.H., Cao, J., Tan, X.C., Luo, B., Zeng, W., Hong, H.T., Huang, X., Wang, Y., 2018. Hydrocarbon generation capability of Sinian–Lower Cambrian shale, mudstone, and carbonate rocks in the Sichuan Basin, southwestern China: implications for contributions to the giant Sinian Dengying natural gas accumulation. AAPG Bull. 102, 817–853. https://doi.org/10.1306/0711171417417019.
Su, A., Chen, H.H., Feng, Y.X., Zhao, J.X., Nguyen, A.D., Wang, Z.C., Long, X.P., 2020. Dating and characterizing primary gas accumulation in Precambrian dolomite reservoirs, Central Sichuan Basin, China: insights from pyrobitumen Re-Os and dolomite U-Pb geochronology. Precambrian Res. 350, 105897. https://doi.org/10.1016/j.precamres.2020.105897.
Su, A., Chen, H.H., Feng, Y.X., Zhao, J.X., Wang, Z.C., Hu, M.Y., Jiang, H., Nguyen, A.D., 2022. In situ U-Pb dating and geochemical characterization of multi-stage dolomite cementation in the Ediacaran Dengying Formation, Central Sichuan Basin, China: constraints on diagenetic, hydrothermal and paleo-oil filling events. Precambrian Res. 368, 106481. https://doi.org/10.1016/j.precamres.2021.106481.
Tan, L., Liu, H., Tang, Q.S., Li, F., Tang, Y.Z., Liang, F., Li, M., Liu, W., 2021. Application of seismic geomorphology to carbonate rocks: a case study of the Cambrian Longwangmiao Formation in the Gaoshiti-Moxi area, Sichuan Basin, China. Mar. Petrol. Geol. 126, 104919. https://doi.org/10.1016/j.marpetgeo.2021.104919.
vS Hood, A., Wallace, M.W., Drysdale, R.N., 2011. Neoproterozoic aragonite-dolomite seas? Widespread marine dolomite precipitation in Cryogenian reef complexes. Geology 39, 871–874. https://doi.org/10.1130/G32119.1.
Wang, Y., Shi, Z., Qing, H.R., Tian, Y.M., Gong, X.X., 2021. Petrological characteristics, geochemical characteristics, and dolomite model of the lower cambrian Longwangmiao Formation in the periphery of the Sichuan Basin, China. J. Petrol. Sci. Eng. 202, 108432. https://doi.org/10.1016/j.petrol.2021.108432.
Wei, G.Q., Yang, W., Xie, W.R., Su, N., Xie, Z.Y., Zeng, F.Y., Ma, S.Y., Jin, H., Wang, Z.H., Zhu, Q.Y., Hao, C.G., Wang, X.D., 2022. Formation mechanisms, potentials and exploration practices of large lithologic gas reservoirs in and around an intracratonic rift: taking the Sinian-Cambrian of Sichuan Basin as an example. Petrol. Explor. Dev. 49, 530–545. https://doi.org/10.1016/S1876-3804(22)60044-2.
Wood, R., Zhuravlev, A.Y., Sukhov, S., Zhu, M., Zhao, F., 2017. Demise of Ediacaran dolomitic seas marks widespread biomineralization on the Siberian Platform. Geology 45, 27–30. https://doi.org/10.1130/G38367.1.
Xiao, D., Cao, J., Luo, B., Tan, X.C., Liu, H., Zhang, B.J., Yang, X., Li, Y., 2020a. On the dolomite reservoirs formed by dissolution: differential eogenetic versus hydrothermal in the lower Permian Sichuan Basin, southwestern China. AAPG Bull. 104, 1405–1438. https://doi.org/10.1306/02262018242.
Xiao, D., Cao, J., Luo, B., Zhang, Y., Xie, C., Chen, S.L., Gao, G.H., Tan, X.C., 2020b. Mechanism of ultra-deep gas accumulation at thrust fronts in the Longmenshan Mountains, lower Permian Sichuan Basin, China. J. Nat. Gas Sci. Eng. 83, 103533. https://doi.org/10.1016/j.jngse.2020.103533.
Xu, Z.H., Lan, C.J., Zhang, B.J., Hao, F., Lu, C.J., Tian, X.W., Zou, H.Y., 2022. Impact of diagenesis on the microbial reservoirs of the terminal ediacaran Dengying Formation from the central to northern Sichuan Basin, SW China. Mar. Petrol. Geol. 146, 105924. https://doi.org/10.1016/j.marpetgeo.2022.105924.
Yan, R.J., Xu, G.S., Xu, F.H., Song, J.M., Yuan, H.F., Luo, X.P., Fu, X.D., Cao, Z.Y., 2022. The multistage dissolution characteristics and their influence on mound-shoal complex reservoirs from the Sinian Dengying Formation, southeastern Sichuan Basin, China. Mar. Petrol. Geol. 139, 105596. https://doi.org/10.1016/j.marpetgeo.2022.105596.
Yang, X.F., Wang, X.Z., Tang, H., Yang, Y.M., Xie, J.R., Luo, W.J., Jiang, N., 2016. Reservoir characteristics and main controlling factors of the Longwangmiao Formation in the Moxi area, central Sichuan Basin, China. Arabian J. Geosci. 9, 1–11. https://doi.org/10.1007/s12517-015-2066-2.
Zhang, Y.G., Yang, T., Hohl, S.V., Zhu, B., He, T.C., Pan, W.Q., Chen, Y.Q., Yao, X.Z., Jiang, S.Y., 2020. Seawater carbon and strontium isotope variations through the late Ediacaran to late Cambrian in the Tarim Basin. Precambrian Res. 345, 105769. https://doi.org/10.1016/j.precamres.2020.105769.
Zhao, W.Z., Shen, A.J., Zheng, J.F., Qiao, Z.F., Wang, X.F., Lu, J.M., 2014. The porosity origin of dolostone reservoirs in the Tarim, Sichuan and Ordos basins and its implication to reservoir prediction. Sci. China Earth Sci. 57, 2498–2511. https://doi.org/10.1007/s11430-014-4920-6.
Zhou, Y., Yang, F.L., Ji, Y.L., Zhou, X.F., Zhang, C.H., 2020. Characteristics and controlling factors of dolomite karst reservoirs of the Sinian Dengying Formation, central Sichuan Basin, southwestern China. Precambrian Res. 343, 105708. https://doi.org/10.1016/j.precamres.2020.105708.
Zhou, Z., Wang, X.Z., Yin, G., Yuan, S.S., Zeng, S.J., 2016. Characteristics and genesis of the (sinian) Dengying Formation reservoir in central sichuan, China. J. Nat. Gas Sci. Eng. 29, 311–321. https://doi.org/10.1016/j.jngse.2015.12.005.
Zhu, G.Y., Wang, T.S., Xie, Z.Y., Xie, B.H., Liu, K.Y., 2015. Giant gas discovery in the Precambrian deeply buried reservoirs in the Sichuan Basin, China: implications for gas exploration in old cratonic basins. Precambrian Res. 262, 45–66. https://doi.org/10.1016/j.precamres.2015.02.023.
Zhu, L.Q., Liu, G.D., Song, Z.Z., Zhao, W.Z., Li, Q., Tian, X.W., Wang, Y.L., Yang, D.L., 2022. Reservoir solid bitumen-source rock correlation using the trace and rare earth elements-implications for identifying the natural gas source of the Ediacaran-Lower Cambrian reservoirs, central Sichuan Basin. Mar. Petrol. Geol. 137, 105499. https://doi.org/10.1016/j.marpetgeo.2021.105499.